



**HAL**  
open science

## Influence of low-frequency variability on groundwater level trends

Lisa Baulon, Delphine Allier, Nicolas Massei, H el ene Bessiere, Matthieu Fournier, Violaine Bault

► **To cite this version:**

Lisa Baulon, Delphine Allier, Nicolas Massei, H el ene Bessiere, Matthieu Fournier, et al.. Influence of low-frequency variability on groundwater level trends. *Journal of Hydrology*, 2022, 606, pp.127436. 10.1016/j.jhydrol.2022.127436 . hal-03558802

**HAL Id: hal-03558802**

**<https://hal.science/hal-03558802v1>**

Submitted on 22 Jul 2024

**HAL** is a multi-disciplinary open access archive for the deposit and dissemination of scientific research documents, whether they are published or not. The documents may come from teaching and research institutions in France or abroad, or from public or private research centers.

L'archive ouverte pluridisciplinaire **HAL**, est destin ee au d ep ot et  a la diffusion de documents scientifiques de niveau recherche, publi es ou non,  emanant des  tablissements d'enseignement et de recherche franais ou  trangers, des laboratoires publics ou priv es.



Distributed under a Creative Commons Attribution - NonCommercial 4.0 International License

# **Influence of low-frequency variability on groundwater level trends**

Lisa Baulon<sup>a,b\*</sup>, Delphine Allier<sup>b</sup>, Nicolas Massei<sup>a</sup>, H el ene Bessiere<sup>b</sup>, Matthieu Fournier<sup>a</sup>, Violaine Bault<sup>b</sup>

<sup>a</sup> Normandie Univ, UNIROUEN, UNICAEN, CNRS, M2C, 76000 Rouen, France

<sup>b</sup> BRGM, 3 av. C. Guillemin, 45060 Orleans Cedex 02, France

\* Corresponding author. [lisa.baulon@etu.univ-rouen.fr](mailto:lisa.baulon@etu.univ-rouen.fr)

## **Abstract**

Estimating groundwater level evolution is a major issue in the context of climate change. Groundwater is a key resource and can even account in some countries for more than half of the water supply. Groundwater trend estimates are often used for describing this evolution. However, the estimated trend obviously strongly depends on available time series length, which may be caused by the existence of long-term variability of groundwater resources. In this paper, using a groundwater level database in Metropolitan France as an example, we address this issue by exploring how much trend estimates are sensitive to low-frequency variability of groundwater levels. Database consists of relatively undisturbed groundwater level time series regarding anthropogenic influence (water abstraction by either continuous or periodic pumping). Frequent changes in trend direction and magnitude are detected according to time series length, which can eventually lead to contradictory interpretations of the groundwater resource evolution, as presented in first part of this article. To assess whether low-frequency variability – known to originate from climate variability – can induce such modifications of trends, we explored in a second step the multi-time scale variability of groundwater levels using a methodology based on discrete wavelet transform. Most of the time series displaying changing trends depending on time series length corresponded to aquifers with high-amplitude low-frequency variability of groundwater levels. Two

27 predominant low-frequency components were detected: multi-annual (~7 years) and decadal (~17  
28 years). We finally examined how much those two low-frequency components may affect trend estimates  
29 on the longer time period available. For this purpose, we individually removed each of both components  
30 from the original times series by discrete wavelet filtering and re-estimated trends in the filtered  
31 groundwater level time series. The results showed that the groundwater level trends were highly  
32 sensitive to the presence of any of these low-frequency components, which may then strongly influence  
33 the estimated trends either by exaggerating or mitigating them. These results emphasize that i)  
34 attributing the estimated trends only to climate change would be hazardous given the large influence of  
35 low-frequency variability on groundwater level trends, ii) estimation of trends in hydrological  
36 projections resulting from GCM outputs in which low-frequency variability is not well represented  
37 would be subject to strong uncertainty, iii) a potential change in the amplitude of internal climate  
38 variability – e.g. increasing or decreasing low-frequency variability – in the next decades may lead to  
39 substantial changes in groundwater level trends.

40

## 41 **Keywords**

42 Low-frequency variability; Groundwater level trends; Metropolitan France; Maximum overlap discrete  
43 wavelet transform

44

## 45 **1. Introduction**

46 According to Iliopoulou and Koutsoyiannis (2020), the number of scientific publications using the word  
47 “trend” has steadily increased over the past two decades, especially in relation to hydroclimatological  
48 variables. Various scientific questions and aims can lead scientists to search for trends in hydrological  
49 processes. The assessment or forecasting of the qualitative and quantitative evolution of environmental  
50 variables – such as detecting short- to long-term increases or decreases – are part of this (Visser et al.,  
51 2009; Giuntoli et al., 2013; Sakizadeh et al., 2019; Caporali et al., 2020; Dudley et al., 2020). These  
52 questions are related to resource preservation issues in the context of global change. For instance, the

53 European Union’s Water Framework Directive is based on this philosophy: detect negative trends in  
54 water resources (streamflow and groundwater levels) with the aim of their protection (European  
55 Commission, 2009); deterioration of a resource can cause restrictions on freshwater withdrawals.

56

57 In the context of climate change, assessing the long-term evolution of hydrological variables and  
58 associated extremes is a major issue, particularly for identifying which parts of this evolution can be  
59 attributed to climate change and to anthropogenic forcing (Massei et al., 2020). For groundwater, this  
60 issue is even more relevant when considering pumping; for instance, groundwater provides 65% of the  
61 water supply in France (Chataigner et al., 2019). Hence, the study of long-term groundwater level  
62 evolution is especially relevant for management purposes and the knowledge of groundwater resource  
63 capacity. Methods for identifying linear or monotonic trends are commonly used for describing changes  
64 in hydrological variables (Stahl et al., 2010; Lorenzo-Lacruz et al., 2012; Blöschl et al., 2019; Pathak  
65 and Dodamani, 2019; Vicente-Serrano et al., 2019; Mohanavelu et al., 2020; Peña-Angulo et al., 2020).

66

67 Although the detection of monotonic trends is a widely used tool for quantifying evolution of  
68 hydrological variables, its use may still raise questions. First, they cannot be extrapolated to other study  
69 periods, and longer or shorter periods, regardless of the type of variable considered (Koutsoyiannis,  
70 2006; Burn and Whitfield, 2018). For a given region, authors commonly find contradictory or varying  
71 results as trends are often not estimated over the same periods, a point that is often discussed as a major  
72 issue (Hannaford et al., 2013; Degefu et al., 2019). Therefore, their “non-extrapolability” makes them  
73 poor predictors and unsuitable for forecasting (Iliopoulou and Koutsoyiannis, 2020). Second, trends  
74 commonly reflect long-range dependence/autocorrelations, because of low-frequency variability in the  
75 hydroclimatic variables of interest (Iliopoulou and Koutsoyiannis, 2020). Such variability generated by  
76 large-scale atmospheric and oceanic circulation patterns is the primary source of a “misperceived” trend,  
77 as short-term periods affected by a trend may actually be part of longer-term fluctuations. Multi-  
78 temporal trend-definition methods have been developed to highlight this dependence of trend  
79 assessment on low-frequency variability (multi-annual–multidecadal) in hydroclimatic variables and to

80 avoid trend “misperceptions” (McCabe and Wolock, 2002; Schmocker-Fackel and Naef, 2010;  
81 Hannaford et al., 2013; Stojković et al., 2014; Peña-Angulo et al., 2020). For instance, Hannaford et al.  
82 (2013) demonstrated that trend direction and magnitude are highly influenced by interdecadal  
83 variability.

84

85 Given the influence of interdecadal variability, and more generally low-frequency variability, on the  
86 hydrological trends, it is crucial to better understand the large-scale origin of these fluctuations and how  
87 catchments can filter and modify them. In this regard, Gudmunsson et al. (2011) indicated that the low-  
88 frequency variability of runoff directly originates from the large-scale atmospheric circulation, while  
89 the catchments properties control the proportion of variance of low-frequency variability in hydrological  
90 variables. Simultaneously, a large amount of studies addressed the large-scale origins of such  
91 variabilities in hydroclimatic variables (streamflow, precipitation, groundwater, temperature), using  
92 climate indices and atmospheric fields (Massei et al., 2010; Boé and Habets, 2014; Dieppois et al., 2013;  
93 Dieppois et al., 2016; Massei et al., 2017; Neves et al., 2019; Liesch and Wunsch, 2019).

94

95 Across the whole metropolitan France area, Fossa et al. (2021) detected ~3-yr and ~7-yr variabilities in  
96 streamflow, precipitation and temperature but with fluctuating amplitudes depending on the region. At  
97 a smaller regional scale, particularly in the Seine watershed, many studies previously highlighted these  
98 same two low-frequency variabilities in precipitation and streamflow as well as a ~17-yr variability  
99 (Massei et al., 2007; Massei et al., 2010; Fritier et al., 2012; Massei and Fournier, 2012; Dieppois et al.,  
100 2013; Massei et al., 2017). The North Atlantic Oscillation (NAO) was described as one significant driver  
101 of such temporal signature (~7-yr and ~17-yr) in precipitation and streamflow (Massei et al., 2007;  
102 Massei et al., 2010). Later, Massei et al. (2017) highlighted using a composite analysis with Sea Level  
103 Pressure (SLP) that the atmospheric pattern associated to the ~7-yr variability was not exactly  
104 reminiscent of the NAO, with centers of action actually shifted to the North. Similarly, the pattern  
105 associated to ~17-yr variability was a spatially extended pattern across the Atlantic ocean with lower  
106 SLP roughly following the Gulf Stream front. This result highlighted that atmospheric patterns

107 associated to ~7-yr and ~17-yr variabilities are not similar and these atmospheric patterns exhibit centers  
108 of action that are not necessarily corresponding to those of established climate indices such as the NAO.  
109

110 Aquifers very often act as rather strong low-pass filters, leading to high-amplitude low-frequency  
111 variability in groundwater levels. In other words, aquifers filter out high-frequency (short-term)  
112 variations of the precipitation input more or less significantly, letting only low-frequency (longer-term)  
113 variations dominate the overall variability of the groundwater level signal. Some studies also  
114 investigated the role played by geological characteristics in controlling the magnitude of these  
115 fluctuations in groundwater levels: thickness of superficial formations, of the vadose zone, hydraulic  
116 properties of aquifers (Slimani et al., 2009; El Janyani et al., 2012; Velasco et al., 2017). In Normandy,  
117 Slimani et al. (2009) and El Janyani et al. (2012) identified a significant ~7-yr variability in groundwater  
118 levels of chalk aquifer consistent with many previous works that had already documented the presence  
119 of both ~7-yr and ~17-yr variabilities, and their link to the NAO in northern France on precipitation  
120 (Massei et al., 2007) or river flow (Massei et al., 2010, 2012, 2017). Later, the exact same multi-annual  
121 and decadal fluctuations were also identified in groundwater levels in Great Britain (Rust et al., 2019)  
122 and on the western European continent (Liesch and Wunsch, 2019; Neves et al., 2019).

123  
124 In this article, we specifically addressed the issue of the influence of low-frequency variability on  
125 groundwater level trend estimates. In metropolitan France, for instance, many changes in trend direction  
126 and magnitude were observed depending on the length of time series considered, thus leading to  
127 completely contradictory conclusions on groundwater level evolutions, as exposed in section 3.1. In  
128 some surface hydrology studies (e.g. Hannaford et al., 2013, as mentioned previously), such  
129 contradictory conclusions were related to low-frequency variability. Therefore as a second step, we  
130 aimed to determine whether French aquifers concerned by these regular changes in trend direction and  
131 magnitude, exhibited a significant low-frequency variability in groundwater levels. In section 3.2., we  
132 thus broke down groundwater level signals using discrete wavelet transform and quantified the variance  
133 percentage of total signal explained by each time scale of variability. Finally, in a third step, we  
134 examined if and how low-frequency variability influenced trend estimates by filtering out each low-

135 frequency component from the original time series using discrete wavelet transform and re-estimating  
136 trends on filtered time series (Section 3.3.). This last point is particularly important because if the low-  
137 frequency variability significantly influences the estimated groundwater level trends, this has several  
138 implications:

- 139 (i) First, regarding the identification of traces of climate change in groundwater levels. Indeed,  
140 if the low-frequency variability in groundwater levels significantly affects trend estimates,  
141 it is hazardous to conclude that, for instance, a decreasing evolution of groundwater levels  
142 is directly the result of climate change. Indeed, such trends would then be primarily the  
143 result of internal climate variability instead of anthropogenic climate change.
- 144 (ii) Second, regarding future projections. Indeed, trend estimates in hydrological projections  
145 resulting from GCM outputs in which low-frequency variability is not well represented  
146 would be subject to strong uncertainty.
- 147 (iii) Third, regarding future evolutions. Indeed, a potential change in the amplitude of internal  
148 climate variability – e.g. increasing or decreasing low-frequency variability – in the next  
149 decades may lead to substantial changes in groundwater level trends.

150

## 151 **2. Data and methods**

### 152 2.1. Data

#### 153 2.1.1. Groundwater data

154 For this study, we used 215 boreholes in continental France, with groundwater level time series being  
155 little or not affected by pumping (Fig. 1). They were selected from a BRGM database on boreholes not  
156 influenced by human activities (Baulon et al., 2020) that was constituted in three steps:

- 157 (i) a selection of boreholes with time series satisfying criteria of duration, minimum amount of  
158 data per month, maximum length of gaps;
- 159 (ii) the crossing of pre-selected boreholes with other BRGM databases on known anthropogenic  
160 influences;

161 (iii) numerous visualisations of time series with the hydrogeologists responsible for piezometric  
162 networks, in order to retain only non-influenced boreholes.

163 Time series of boreholes in this database were initially gathered in the ADES database that contains all  
164 groundwater data (quantity and quality) across continental France (<https://ades.eaufrance.fr/>).

165

166 *Figure 1. Spatial distribution of the 215 little- or non-influenced groundwater boreholes in*  
167 *continental France*

168

169 The criteria satisfied for selecting groundwater level time series in the database, and thus for the present  
170 study, were:

- 171 • The duration of the groundwater level time series must be >30 yr for regions where monitoring  
172 history is sufficiently long, and >20 yr for regions where monitoring history is shorter.
- 173 • The time series must contain a minimum amount of data in a month. This minimum amount is  
174 divided into two parts. A date of sampling-frequency change is identified in each time series,  
175 and the minimum sampling frequency must be at least one datum per month before this date  
176 and three data per month after this date.
- 177 • The length of consecutive gaps must be <3 yr for time series starting after 1950 and <10 yr for  
178 time series starting before 1950. This allows time series in the new database to preserve low-  
179 frequency variability in the data. Several gaps in the time series can be allowed if these criteria  
180 are respected, and if the number of gaps and their lengths are small.

181 Before data analysis, a visual check of the groundwater level time series served to remove or correct  
182 erroneous data. Wishing to qualify the behaviour of water tables by including annual variability, we  
183 decided to work on monthly averages. Any missing months in these time series were then filled by linear  
184 interpolation, before spectral analyses.

185

186 In continental France, groundwater level time series in some regions span on a limited historical time  
187 period, especially in western and southern France. Hence, we decided to focus on two different time  
188 spans: 1996–2019 and 1976–2019. For all French aquifers, the analyses cover the 1996–2019 period,



189 ensuring a good trade-off between time series length and spatial coverage (215 time series available).  
190 The longer period, spanning 43 years between 1976 and 2019, covered 102 time series in northern  
191 France. These two periods are referred to as “reference periods”.

192

193 In our study, the selected wells are representative of the various French hydrogeological contexts:  
194 alluvial, sedimentary, volcanic, and bedrock aquifers, but most wells are in sedimentary aquifers,  
195 primarily in the Paris Basin, and some in the Aquitaine Basin. Each well is attached to a hydrogeological  
196 area based on the groundwater bodies.

197

198 In the resulting database, the Seno–Turonian chalk aquifer of the Paris Basin is the best represented (60  
199 boreholes), followed by Jurassic limestone aquifers in Lorraine, Berry, and Poitou on the rim of the  
200 Paris Basin (19 boreholes), and the Eocene Beauce limestones aquifer (8 boreholes). Wells in the  
201 Aquitaine Basin mainly capture the Jurassic limestone aquifer of the northern part of the Basin (7  
202 boreholes) and multiple sedimentary hydrogeological formations in the southern part (sand, limestone:  
203 10 boreholes). Finally, most of the wells selected in the Rhône valley monitor alluvial and fluvio-glacial  
204 formations (11 boreholes).

205

206 Alluvial aquifers are also well represented in the dataset, especially the Rhine/Vosges alluvium (18  
207 boreholes) in Alsace, the Garonne alluvium in the Toulouse region (3 boreholes), and recent alluvium  
208 in the Mediterranean region (11 boreholes).

209 Some wells in the Central Massif are located in volcanic aquifers in various formations with different  
210 behaviour of groundwater levels (5 boreholes). Finally, bedrock aquifers are monitored by a few selected  
211 wells in the Armorican Massif (10 boreholes).

212

### 213 2.1.2. Precipitation data

214 Precipitation data used in this study come from the SAFRAN reanalysis (Vidal et al., 2010), which  
215 provides daily data on an 8×8 km<sup>2</sup> mesh covering France from 1958 to 2019. In addition, based on

216 meteorological data (precipitation (P), snow, temperature, and Penman-Monteith potential  
217 evapotranspiration (PET)) from the SAFRAN reanalysis, effective precipitation ( $EP = P - PET$ ) data  
218 were computed using a gridded water-budget model with 8 km resolution at a daily time step, relying  
219 on the water-budget method of Edijatno and Michel (1989). The water-budget method considers that  
220 in the water cycle, the soil acts as a reservoir characterized by its water storage capacity. Edijatno and  
221 Michel (1989) introduced a quadratic law to progressively empty the soil water reserves and to distribute  
222 the positive difference between P and PET between EP and soil storage. In the present study, the  
223 temporal resolution of both precipitation and effective precipitation was set at a monthly time step by  
224 using monthly cumulated data.

225

## 226 2.2. Methods

### 227 2.2.1. Trends over multiple time series lengths

228 We first estimated groundwater level trends over multiple time series lengths. We then determined  
229 whether changes in the length of time series affected trend estimates, by assessing the stability of trends  
230 when comparing the direction and magnitude of trends over decreasing periods. The procedure is  
231 illustrated in Fig. 2a. As explained above, we split the trend stability analysis into two reference periods,  
232 1976–2019 and 1996–2019, corresponding to the best agreements between the spatial distribution of  
233 wells and groundwater level time series lengths over northern aquifers (102 boreholes) and all of  
234 continental France (215 boreholes), respectively. The 1996–2019 reference period provided an image  
235 of the stability of groundwater level trends through whole continental France, though over a relatively  
236 short period. To improve the consistency of the study, the 1976–2019 reference period was used for  
237 obtaining a longer historical hindsight, but covering only northern aquifers due to the data availability.

238

239 **Figure 2.** Workflow of (a) trend stability analysis over decreasing time periods and (b) assessment of  
240 groundwater low-frequency influence on trend direction and magnitude. “WLF” is “water level  
241 fluctuation”.

242

243 To complete the stability analysis, we first evaluated the magnitude of trends and their statistical  
244 significance over different study periods (Fig. 2a; Step 1). Within the 1976–2019 reference period,  
245 trends were estimated for all groundwater level time series over six periods: 1976–2019, 1981–2019,  
246 1986–2019, 1991–2019, 1996–2019 and 2000–2019. Within the 1996–2019 reference period,  
247 groundwater level trends were estimated over two study periods: 1996–2019 and 2000–2019. The  
248 significance of monotonic trends was determined with a modified Mann–Kendall trend test for  
249 autocorrelated data (Hamed and Ramachandra Rao, 1998). Compared to the well-known Mann–Kendall  
250 trend test (Mann, 1945; Kendall et al., 1987), the modified Mann–Kendall trend test considers  
251 autocorrelation by correcting probability values (p-values) after accounting for autocorrelation. The  
252 threshold for statistical significance was set at 5%. As we primarily aimed at quantifying changes in  
253 groundwater level trends in relation to groundwater stock variation over decreasing time periods – which  
254 cannot be estimated by the significance value of the modified Mann–Kendall trend test – we developed  
255 an indicator describing this phenomenon. Therefore, although the statistical significance of trends was  
256 also tested in the present study, we decided to present only the afore-mentioned indicator.

257

258 To develop this indicator, we first assessed the magnitude of trends by estimating Sen’s slope (Sen,  
259 1968), this method was selected as it is less sensitive to outliers than linear regression. The slope is  
260 defined as the median of the set of slopes calculated between pairs of points. To evaluate the relative  
261 importance of trends, compared to the groundwater stock variation, the percentage of decrease or  
262 increase in groundwater levels compared to the maximum water level fluctuation (WLF) was calculated  
263 using the following equation:

$$264 \quad \text{Percentage of maximum WLF} = \left( \frac{\text{Sen's slope} * \text{duration}}{\text{Maximum WLF}} \right) * 100 \quad (1)$$

265 where maximum WLF is the difference between the highest and the lowest groundwater levels measured  
266 for a given time series. This normalisation of Sen’s slope by the maximum WLF allowed comparing the  
267 magnitude of groundwater trends between aquifers with various water table behaviours and significant  
268 differences in their water stock variations.

269

270 The percentages of groundwater level loss/gain against maximum WLF were split into five classes  
271 according to their magnitude:

- 272 • Negligible trends between -1% and +1% of maximum WLF;
- 273 • Moderate upward or downward trends between +1% and +10%, or -1% and -10%, of the  
274 maximum WLF, respectively;
- 275 • Strong upward or downward trends between +10% and +100%, or -10% and -100%, of the  
276 maximum WLF, respectively.

277 This normalisation was applied to every well for each period analysed. The maximum WLF adopted,  
278 i.e. that of the two reference periods, remained constant from one period to the next, as it is a parameter  
279 that we used for characterising the groundwater stock variation.

280

281 For each well, the trend stability was evaluated by comparing the trend direction and belonging to the  
282 above classification for all studied periods (Fig. 2a; Step 2). For a given borehole, the groundwater trend  
283 can be stable or unstable in direction. We considered a trend direction “stable” if its direction was  
284 constantly upward, downward, or negligible from one period to another. Conversely, a trend was  
285 “unstable” when its direction fluctuated depending on the study period, or whether a trend emerged,  
286 such as a negligible trend for a given period followed by an upward or downward trend for the next  
287 period. Moreover, a “direction-stable” trend can be stable or unstable in magnitude; it is stable when the  
288 magnitude class does not change between periods and unstable if it does change.

289

### 290 2.2.2. Groundwater multi-timescale variability analysis

291 To determine the importance of low-frequency variability in groundwater levels, we identified and  
292 extracted high- to low-frequency wavelet components by multiresolution analysis, using the maximum  
293 overlap discrete wavelet transform (MODWT) algorithm. Like the more common discrete wavelet  
294 transform (DWT) method, MODWT is an iterative filtering of time series using a series of low- and  
295 high-pass filters, producing one high-frequency component, or “wavelet detail”, and one lower  
296 frequency component called “approximation” or “smooth” at each scale. The smooth component is then

297 further decomposed into a wavelet detail and a smooth component, the latter being decomposed again  
298 until it can no longer be decomposed. The original signal can be reconstructed by summing up all the  
299 wavelet details and the last smooth. The original signal is then separated into a relatively small number  
300 of wavelet components from high to low frequencies, which together explain the total variability of the  
301 signal. For this study, the maximum decomposition level used in the MODWT was  $\log_2(N)$  where  $N$  is  
302 the length of the time series. The least-asymmetric (symmlet) wavelet “s20” was used in order to better  
303 capture variability at all time scales of sometimes relatively smooth groundwater level time series.

304

305 However, unlike DWT, MODWT was essentially designed to prevent phase shifts in the transform  
306 coefficients at all scales by avoiding downsampling – reducing by a factor 2 the number of coefficients  
307 – the signal with increasing scales. It results that the computed wavelet and scaling coefficients at each  
308 scale remain aligned with the original time series; that is, the variance explained by these coefficients is  
309 located where it truly lies in the time series analysed (Percival and Walden, 2000; Cornish et al., 2003;  
310 Cornish et al., 2006). While not necessarily essential for signal or image processing or numerical  
311 compression, this property is fundamental for physical interpretation of the wavelet details in  
312 multiresolution analysis, and has already been used to that purpose in several studies such as Percival  
313 and Mofjeld (1997), Massei et al. (2017) and Pérez Ciria et al. (2019).

314

315 The dominant frequency associated with each MODWT wavelet detail was calculated by Fourier  
316 transform of each wavelet detail. The MODWT also provides the amount of variance (or energy)  
317 explained by each wavelet detail and frequency level. The energy percentage of a given wavelet detail  
318 expresses the relative importance of this variability in the total signal variability. As a result, the energy  
319 distribution between wavelet details for each well in the database can be extracted and mapped.

320

321 Continuous global wavelet spectra were also calculated by averaging the spectral power from the  
322 continuous wavelet spectra over time (Torrence and Compo, 1998). These analyses used R packages  
323 *wmtsa* (Constantine and Percival, 2016) and *biwavelet* (Gouhier and Grinsted, 2012). They were  
324 conducted for both reference periods: 1976–2019 and 1996–2019.

325  
326  
327  
328  
329  
330  
331  
332  
333  
334  
335  
336  
337  
338  
339  
340

2.2.3. Influence of low-frequency variability of groundwater levels on trend direction and magnitude

The influence of groundwater low-frequency variabilities on the trend direction and magnitude was estimated using the MODWT method. As described in Section 2.2.2., summing up all wavelet details and the last smooth rebuilds the original signal. Based on this assessment, we first subtracted the wavelet detail of interest (or component) corresponding to a specific variability from the original signal (i.e., groundwater level monthly averages) (Fig. 2b; Step 1). We then calculated the Sen’s slope (Section 2.2.1.) of the filtered signal and normalised it to the maximum WLF of the original signal (i.e., without filtering) (Fig. 2b; Step 2). The interest in keeping a fixed maximum WLF to normalise Sen’s slopes is to assess only the influence of the removal of the component on the slope, and not to assess the influence of the removal of the component combined to variance modification linked to the removal of the component. Finally, we compared the magnitude and direction of the trends between the original and filtered signals to assess the influence of the component on the trend of the original signal. This analysis covered both reference periods: 1976–2019 and 1996–2019.

341 **3. Results**

342 3.1. Stability of trend directions and magnitudes of groundwater levels

343 In this section, we investigate the stability of groundwater level trends, that is, we aim at determining if  
344 trend direction and magnitude change according to the length of time series used for the trend analysis.  
345 To this end, we introduce the notions of “trend stability” (no change in direction or magnitude) and  
346 “instability” (changes in direction or magnitude) over decreasing time periods. If trend direction is  
347 stable, we consider that the length of time series has a minor influence on trend estimate, then a  
348 conclusion about groundwater level evolution may be drawn. Conversely, if it is unstable, the time series  
349 length has a significant influence on such estimate, then any conclusion regarding groundwater level

350 evolution may not be drawn. The trend-stability maps for the reference periods (1976–2019 and 1996–  
351 2019) used to verify this hypothesis, are shown on Figure 3.

352

353 **Figure 3.** *Trend-stability maps from the two reference periods (a) 1976–2019 to 2000–2019 and (b)*  
354 *1996–2019 to 2000–2019. These maps show for a given reference period to what extent groundwater*  
355 *level trends are susceptible to changes of direction and magnitude according to the time series length.*  
356 *If the change of time series length does not affect trend direction (stable trend in direction), a triangle*  
357 *or a square is drawn for the borehole. If the change of time series length affects trend direction*  
358 *(unstable trend in direction), a diamond or a crossed-out circle is drawn according the type of trend*  
359 *instability. Finally, if the change of time series length does not affect trend magnitude (stable trend in*  
360 *magnitude), a dot is added in the symbol.*

361

362 From the 1996–2019 reference period, some hydrogeological formations show an instability in trend  
363 direction (positive and negative trend; Fig. 3b). These instabilities in trend direction are represented on  
364 maps either with a diamond in case of change of sign from a period to another period (alterning positive  
365 and negative trend) or a crossed-out circle in case of emerging trend (insignificant trend and positive or  
366 negative trend). These entities are the Eocene Beauce limestones, the Seno–Turonian chalk of Artois–  
367 Picardy (Fig. 4; Beauval), and the Jurassic limestones from Sarthe to Bessin. For these entities, no  
368 conclusions regarding the evolution of groundwater levels can be drawn, given the recurrent change in  
369 trend direction according to the length of time series taken into account for the trend analysis.

370

371 **Figure 4.** *Example of trends over multiple time series lengths (1996–2019 and 2000–2019) on*  
372 *monthly groundwater levels at Beauval (Seno-Turonian chalk of Artois-Picardy), Goupillières (Seno-*  
373 *Turonian chalk of Normandy/Picardy) and Penol (fluvio-glacial formations in Rhône valley).*

374

375 Conversely, the Seno–Turonian chalk of Normandy/Picardy (Fig. 4; Goupillières), the Jurassic  
376 limestones of Poitou and Berry, the fluvio-glacial formations of the Rhône valley (Fig. 4; Penol), the  
377 Brittany bedrock, Champagne and Bourgogne chalk exhibit stable trend directions (Fig. 3b). For these

378 entities, conclusions regarding groundwater level evolution may be drawn: they are still downward  
379 regardless the study period.

380

381 However, if the analysis is conducted over longer periods for hydrogeological entities of northern France  
382 (particularly for the Normandy/Picardy, Champagne and Bourgogne chalk), changes in trend direction  
383 or a trend emergence can be detected when changing the time series length (Fig. 3a). Consequently,  
384 conclusions regarding the groundwater level evolution drawn for the 1996–2019 reference period are  
385 no longer valid for the 1976–2019 reference period since instabilities in trend direction are detected.  
386 Naturally, boreholes with trend direction instability between 1996–2019 and 2000–2019 periods are also  
387 subject to this instability over longer periods. Overall, the result is not homogeneous within the same  
388 hydrogeological unit as we can detect both boreholes with stable and unstable trend directions.

389

390 Most boreholes with stable (upward or downward) trend directions from the shorter reference period  
391 (1996–2019) are also stable in magnitude, meaning that the importance of slope in relation to  
392 groundwater level amplitude does not change class (Fig. 3b – dot in the symbol). This is the same for  
393 the longer reference period (1976–2019) in the western Seno-Turonian chalk of Normandy and the  
394 Lutetian/Ypresian sands of the Paris Basin (Fig. 3a).

395

396 Overall, when stable trend directions are detected, from the reference period 1976–2019 for northern  
397 France and 1996–2019 for the other regions of France, and that conclusions on groundwater level  
398 evolutions can be drawn, the levels are in the majority decreasing (Fig. 3). The existence of unstable  
399 trend directions raises the following question: are there low-frequency variabilities in groundwater  
400 levels that could induce these changes in trend directions and thus influence the trend estimates?  
401 Consequently, next section aims to identify the existence and significance of low-frequency variability  
402 in groundwater level signals.

403



### 404 3.2. Groundwater level fluctuations across multiple timescales: significance and spatial 405 distribution over France

406 In this section, we assess the existence, significance and spatial distribution of low-frequency variability  
407 in groundwater level signals over France. We aim at determining if the unstable trend directions  
408 previously identified, could be potentially induced by the existence of low-frequency variability in  
409 groundwater level signals.

410

411 The energy percentage (i.e., the proportion of the total variance) at each timescale of variability can be  
412 extracted via MODWT and mapped for each groundwater time series. Figure 5 shows the spatial  
413 distribution of the energy contained in each spectral component, as a function of the hydrogeological  
414 entity. Multi-annual (5–12 yr) and decadal (12–24 yr) variabilities dominate over much of the Paris  
415 Basin (from Beauce limestones to the Seno–Turonian chalk farther north). Elsewhere, low-frequency  
416 variability can also prevail over a short period (1996–2019), such as in the fluvio-glacial formations of  
417 the Rhône basin, the Jurassic limestones of Poitou, and the alluvial formations of the Garonne River.  
418 Increasing the length of the studied period (1976–2019) highlights the prevalence of decadal variability  
419 (12–24 yr) in groundwater levels in the Beauce limestones and in the southern Seno–Turonian chalk of  
420 Normandy. This decadal variability also occurs in significant proportions farther north in the Seno–  
421 Turonian chalk of Normandy, but there its proportion is rather similar to that of the multi-annual  
422 variability (5–12 yr). These observations highlight the inertial nature of water tables in Normandy chalk  
423 and Beauce limestones aquifers (Fig. 6a and 6b) due to their highly capacitive nature, particularly in  
424 plateau areas (Roux, 2006). In these hydrogeological units, groundwater levels depend essentially on  
425 recharge from past winters. They are particularly sensitive to a succession of dry or wet winters, due to  
426 the memory effect linked to the regulation power of the water table. Regeneration of the water table  
427 stock spans several successive years with excess winter recharges.

428

429 **Figure 5.** *Proportion of the total variance explained by each timescale of variability (energy*  
430 *associated to each timescale, expressed as the percentage of total energy of each groundwater time*  
431 *series).*

432  
433 **Figure 6.** *Examples of groundwater level time series representative of each major water tables*  
434 *behaviour.*

435  
436 Although these low-frequency variabilities (multi-annual and decadal) are substantial components of  
437 the total groundwater variability in the Seno–Turonian chalk of the Artois–Picardy region, the annual  
438 variability explains a larger part of the total groundwater variability than in Normandy and Picardy (Fig.  
439 5). The groundwater levels on the borders of the Seno–Turonian chalk (Champagne and Bourgogne)  
440 also display this type of variability, but here the annual variability dominates. Jurassic limestones on the  
441 edge of the Paris Basin from the Lorraine region to the Berry region also show this predominant annual  
442 variability with only a small part of the total variability explained by multi-annual and decadal  
443 variabilities. Overall, the water tables in these hydrogeological units show a combined behaviour:  
444 variously significant multi-annual to decadal variability is superimposed by prominent annual variability  
445 (Fig. 6c and 6d). In these aquifers, the annual variability is all the more important as their storage  
446 capacity decreases, with increasing fracturing, permeability, and proximity to the outlet (Roux, 2006).  
447 Here, groundwater levels strongly depend on infiltrated rainfall during the previous winter, while having  
448 a memory effect linked to the regulation power of water table.

449  
450 Annual variability generally becomes predominant in compact highly fractured and low capacitive  
451 sedimentary aquifers (Roux, 2006), such as the fissured Jurassic limestones of the northern Aquitaine  
452 Basin or in fractured bedrock of Brittany (Fig. 5b and 6e). In such settings, groundwater levels rapidly  
453 rise in response to winter rainfall, but drop as rapidly as soon as water input stops.

454  
455 No typical pattern in the energy distribution is noticeable for alluvial aquifers in France, and the  
456 dominance of one variability compared to another strongly depends upon the local geological and

457 hydrological context (Fig. 5). Boreholes monitoring alluvial formations commonly also monitor the  
458 underlying water body in the absence of an impermeable layer. Consequently, the borehole captures the  
459 behaviours exhibited by both groundwater bodies. Hence, water tables in alluvial formations can exhibit  
460 either an annual, multi-annual, or combined behaviour.

461  
462 Hydrogeological entities previously described as susceptible to trend direction instabilities, are  
463 essentially entities for which the water tables display inertial or combined behaviour, which means that  
464 the existence of a low-frequency variability in groundwater levels and in significant proportions could  
465 be partly responsible for these instabilities (Fig. 3 and 5). These entities are: the Normandy/Picardy  
466 chalk, the Artois-Picardy chalk, the Bourgogne and Champagne chalk, the Beauce limestones, and the  
467 southern Jurassic limestones from Sarthe to Bessin.

468  
469 The superposition of all the global wavelet spectra calculated for each groundwater level time series  
470 gives us a synthetic view of the predominant variabilities in groundwater levels of French aquifers (Fig.  
471 7). The three preeminent variabilities in monthly groundwater levels are: ~1 yr, 5–8 yr (~7-yr), and >12  
472 yr (~17-yr). The ~7-yr and ~17-yr variabilities show larger spectral powers and carry the largest part of  
473 the low-frequency variability in monthly groundwater levels. Such characteristic variabilities are known  
474 to be induced by large-scale climatic circulation, including the NAO, and was earlier observed in  
475 Normandy groundwater levels by Slimani et al. (2009) and El Janyani et al. (2012), and in streamflow  
476 of the Seine River (Massei et al., 2010). Later, studies highlighted these variabilities in groundwater  
477 levels in other countries (Rust et al., 2019; Liesch and Wunsch, 2019; Neves et al., 2019).

478  
479 **Figure 7.** *Global wavelet spectra of (a) 102 monthly groundwater levels over 1976–2019, covering*  
480 *northern France and (b) 215 monthly groundwater levels over 1996–2019, covering all of France.*

481 *Leading variabilities are highlighted.*

482  
483 Since the low-frequency variabilities significantly explain groundwater level variability, the next section  
484 seeks to determine if, how and to what extent they influence the estimated trends on the reference

485 periods. As the ~7-yr and ~17-yr variabilities appear to be the predominant low frequencies in  
486 groundwater level signals, hereafter, we provide details on the influence of these two variabilities on  
487 groundwater level trends.

488

### 489 3.3. Influence of groundwater level low-frequency variability on trend direction and 490 magnitude

491 In this section, we aim at determining the influence of groundwater multi-annual (~7-yr) and decadal  
492 (~17-yr) variabilities on the estimated trends. In other words, we want to determine whether these low-  
493 frequency variabilities affect trend estimates, and if so, whether they aggravate or mitigate the estimated  
494 trends on the reference periods. To this end, we individually removed the detected low-frequency  
495 components corresponding to multi-annual and decadal variabilities and recomputed the trends for the  
496 resulting filtered groundwater level signals, to assess the effect of such low-frequency components on  
497 trend magnitude and direction. Low-frequency components to be filtered were chosen based on global  
498 wavelet spectra (Fig. 7). For the 1996–2019 reference period, only the ~7-yr component was filtered  
499 from monthly groundwater levels, while for the 1976–2019 reference period, both ~7-yr and ~17-yr  
500 components were individually filtered (Fig. 8 and 9).

501

502 **Figure 8.** Comparison of groundwater trend magnitude between monthly groundwater levels and ~7-  
503 yr filtered groundwater levels over 1996–2019.

504

505 **Figure 9.** Comparison of groundwater trend magnitude between monthly groundwater levels, ~7-yr  
506 filtered groundwater levels, and ~17-yr filtered groundwater levels over 1976–2019. The legend of  
507 hydrogeological entities can be found on Fig. 8.

508

509 Figures 8 and 9 show the magnitude of the trend (Sen's slope/maximum WLF ratio) of each groundwater  
510 time series analysed. Monthly groundwater levels are in red, the ~7-yr filtered monthly groundwater  
511 levels in grey, and the ~17-yr filtered groundwater levels in blue (only for the 1976–2019 period). Both

512 figures show the impact of removing a given variability (~7-yr or ~17-yr) on the trend, compared to the  
513 unfiltered groundwater levels; they also show the influence of a given low-frequency variability on  
514 unfiltered groundwater level trends by considering the sign of the subtraction between unfiltered (red)  
515 and filtered (grey or blue) groundwater levels. Nevertheless, quantifying the exact contribution of a  
516 given variability to unfiltered groundwater level trends is difficult because other (low- or high-  
517 frequency) variabilities can modulate this contribution.

518

519 For the shorter period (1996–2019), the effect of the ~7-yr variability on trends shows a well-established  
520 spatial pattern throughout France (Fig. 8). In the North, for aquifers with inertial or combined behaviour  
521 of water tables, the ~7-yr variability drives levels up. In contrast, in various southern French aquifers,  
522 this variability drives groundwater levels down.

523

524 In northern France in chalk, sands, and Eocene limestones of the Paris Basin, we see an accentuation of  
525 downward trends (Fig. 10b; Goupillières), a mitigation of upward trends, and reversals in direction from  
526 upward to downward trends when the ~7-yr variability is filtered from monthly groundwater levels (Fig.  
527 8b1). This effect of removing the ~7-yr variability means that in unfiltered original groundwater levels,  
528 this variability drives groundwater levels upward. In other words, the ~7-yr variability mitigates  
529 downward trends and accentuates upward trends. The Seno-Turonian chalk of Champagne is the only  
530 one not displaying this phenomenon. Around the hydrogeological entities of the Paris Basin, the effect  
531 of the ~7-yr variability on groundwater levels is more sporadic.

532

533 **Figure 10.** *Typical patterns of low-frequency variability removal influence on groundwater level trend*  
534 *estimates: (a) Analysis of the 1976–2019 period at Goupillières (Seno-Turonian chalk of Normandy*  
535 *and Picardy) and Beauval (Seno-Turonian chalk of Artois-Picardy) both in northern France; (b)*  
536 *Analysis of the 1996–2019 period at Goupillières (northern France) and Penol (southern France –*  
537 *fluvio-glacial formations of Rhône valley).*

538

539 In southern France, we see a reverse pattern from that found in the North (Fig. 8). Here, removing the  
540 ~7-yr variability mitigates downward trends (Fig. 10b; Penol), or results in downward trends becoming  
541 upward trends (Fig. 8b2). This pattern is observed in all southern hydrogeological units analysed, even  
542 if locally the removal of the ~7-yr variability may have no effect on the trends. This “non-effect” could  
543 be caused either by the fact that the ~7-yr variability does not, or weakly explain, the variability of  
544 monthly groundwater levels, or because this variability does not contribute to the trend at all. Overall,  
545 the ~7-yr variability drives groundwater levels down in most southern hydrogeological entities. In other  
546 words, the ~7-yr variability aggravates downward trends.

547

548 A transitional section between northern and southern patterns can be seen in the Jurassic limestones of  
549 Berry (Fig. 8). Here, the ~7-yr variability can drive groundwater levels upward or downward. This  
550 transition zone could be attributed to either a transitional climatic zone, or a high spatial variability in  
551 water table behaviour, related to a spatial discrepancy of aquifer properties.

552

553 The ~7-yr variability displays a similar pattern for the longer period (1976–2019) as for the shorter one  
554 in the Paris Basin (Fig. 9b). Removing this variability still results in accentuated downward or mitigated  
555 upward trends. The main discrepancy compared to the shorter period is due to the fact that, in many  
556 cases, removing the ~7-yr variability hardly affects the trend (Fig. 10a; Goupillières and Beauval).  
557 Hence, the ~7-yr variability either drives groundwater levels upward, so mitigates downward trends, or  
558 has no effect on the trend in the Paris Basin. The Seno–Turonian chalk of Champagne also displays this  
559 pattern, while the Upper Cretaceous chalk of Bourgogne does not.

560

561 The long reference period allows for a robust assessment of the influence of the ~17-yr variability on  
562 groundwater trends (Fig. 9), as it shows a consistent pattern in hydrogeological units of northern France,  
563 driving groundwater levels downward, so aggravating downward trends. The removal of this variability  
564 leads to mitigation of downward trends (Fig. 10a; Goupillières), accentuation of upward trends, or  
565 reversals in trend directions from downward to upward. The only hydrogeological unit where the ~17-

566 yr variability does not influence the trend is the Seno–Turonian chalk of Artois–Picardy (Fig. 10a;  
567 Beauval).

568

569 Figure 10a also shows the importance of the ~17-yr variability weakening since the late 2000s in  
570 carrying trend: the trend is largely mitigated when this variability is removed from the monthly  
571 groundwater levels at Goupillières. At Beauval, this is not the case, because the ~17-yr variability only  
572 accounts for a small part of total variability, and therefore has no influence on the trend.

573

574 The degree of influence of a specific variability on the trend can be related to two factors: (i) the  
575 proportion of total groundwater variability explained by this variability and (ii) the length of the time  
576 series. The greatest influence on trends of removing a specific variability occurs when it accounts for a  
577 large part of the total groundwater variability. This phenomenon is particularly remarkable in inertial  
578 formations. For instance, removing the ~7-yr variability over the 1996–2019 period strongly affects  
579 groundwater level trends in Beauce limestones, Seno–Turonian chalk, and fluvio-glacial formations in  
580 the Rhône valley (Fig. 8). As seen earlier, the ~7-yr variability explains much of the total groundwater  
581 variability in these units over the 1996–2019 period (Fig. 5b).

582

583 Similarly, removing the ~17-yr variability over the 1976–2019 period strongly affects groundwater level  
584 trends in Beauce limestones and southern Seno–Turonian chalk of Normandy (south of the Seine River),  
585 while this influence weakens farther north until it no longer affects trends in the Seno–Turonian chalk  
586 of Artois–Picardy (Fig. 9). This weakening pattern corresponds to a decrease in the significance of the  
587 ~17-yr variability in monthly groundwater variability from the Beauce limestones to the Seno–Turonian  
588 chalk of the Artois–Picardy basin farther north (Fig. 5a).

589

590 In addition to the explanatory variance, the other major factor that affects the importance of a given  
591 variability removal on trends magnitude and direction is the length of the time series. Thus, removing  
592 the ~7-yr variability over a long period (1976–2019) has less influence on trends than over a shorter  
593 period (1996–2019). We see an example of this in the northern part of the Seine River, in the Seno–

594 Turonian chalk of Normandy. During the 1976–2019 period, the ~7-yr variability still explains half of  
595 the groundwater level variability (Fig. 5a), but its removal from groundwater levels hardly affects trends  
596 (Fig. 9).

597

## 598 **4. Discussion**

599 In this section, we discuss the different items addressed in the section 3. First, we discuss how the length  
600 of groundwater time series can influence trend estimation and thus conclusions regarding groundwater  
601 level evolution. We also discuss to what extent it may be related to the presence of low-frequency  
602 variability in groundwater signals, and to what extent the length of groundwater time series is a key  
603 parameter to determine the trend origin. By trend origin, we refer to the physical phenomenon that leads  
604 to the groundwater level trend. Second, we discuss the presence of low-frequency variability in  
605 groundwater levels and the relationship with aquifer and catchments properties. Finally, we discuss the  
606 influence of multi-annual and decadal variabilities on groundwater trends and compare these results to  
607 those obtained for (effective) precipitation with the aim to determine whether these influences originate  
608 from precipitation or whether catchment and aquifer properties disrupt these influences. Furthermore,  
609 we develop the implications of such results on the interpretation of estimated groundwater level trends  
610 as well as on future evolutions and projections of groundwater levels.

611

### 612 **4.1. Importance of time series length on trend estimates and to discuss the origin of** 613 **groundwater trends**

614 A few studies have previously examined the influence of time series length on the magnitude and  
615 statistical significance of hydroclimatic variable trends. It emerged that the shorter the study period, the  
616 greater its magnitude and statistical significance, which appeared to be directly linked to low-frequency  
617 variability (Hannaford et al., 2013; Peña-Angulo et al., 2020). The low-frequency variability also  
618 interferes in the statistical test results with high magnitude trends that may be statistically insignificant  
619 but may actually have important implications for water resources (Morin, 2011; Fatichi et al., 2015a).



620 The main method for mitigating the effect of multi-annual and multidecadal variabilities on trends is to  
621 lengthen the study period as much as possible (Peña-Angulo et al., 2020). However, the main limitation  
622 to lengthen the study period comes from the existence of historical data. In our case, the French  
623 piezometric network is relatively young, which constrains trend studies to be realised on short periods.  
624 Therefore, as much studies (Burn et al., 2012), our trend study is conducted using temporal windows  
625 that provide the best compromise between time series length and the spatial coverage of *in situ* stations.

626

627 We showed that some aquifers exhibiting inertial or combined behaviour of water tables are particularly  
628 susceptible to trend direction instabilities (alternatively upward and downward) when the length of  
629 groundwater time series is modified. It is therefore difficult to draw a conclusion on the groundwater  
630 level evolution. Shifting trend directions are not specifically inherent to groundwater levels but can also  
631 be observed in streamflow and precipitation (Hannaford et al., 2013; Stojković et al., 2014; Espinosa  
632 and Portela, 2020; Peña-Angulo et al., 2020). Such trends should be interpreted with great care, as they  
633 may actually correspond to the presence of low-frequency variability, and do not represent a physically  
634 meaningful trend behaviour, i.e., a change in the behaviour of the analyzed phenomenon that may  
635 eventually lead to a new (yet unknown) state, for instance as a consequence of anthropogenic climate  
636 change or changes in land use.

637

638 However, the existence of significant low-frequency variability in groundwater levels does not  
639 necessarily induce trend direction instabilities, as it was observed for some aquifers exhibiting water  
640 tables with inertial or combined behaviour. In such case with still upward or downward trends regardless  
641 the time series length, conclusions about groundwater level evolution may be drawn. Nevertheless,  
642 observing still upward or downward trends does not allow us to deduce the origin of the trend. For  
643 instance, the detected decreasing trends may be induced either by (i) the anthropogenic climate change  
644 resulting in a decrease in groundwater recharge, (ii) the internal climate variability (developed in  
645 subsequent paragraphs), or (iii) anthropogenic impacts (e.g., groundwater pumping, changes in land  
646 cover that may generate a decrease in groundwater recharge).

647

648 Internal climate variability (i.e. the low-frequency variability) may lead to stable trend directions in  
649 different ways according our observations (not exhaustive). First, since low-frequency variability  
650 displays an aperiodic behaviour with regular amplitude-modifications, consequently trends may be  
651 largely guided by these amplitude-modifications of low-frequency that may lead to a trend direction still  
652 upward or downward regardless the length of time series considered (developed in Section 4.3.). Second,  
653 trends detected over relatively short periods may actually be only sections of slower fluctuations.  
654 Consequently, the trend direction remains upward or downward regardless the time series length  
655 considered, since the available length of groundwater level time series is still too short to grasp certain  
656 low-frequency timescales as fluctuations, but they are grasped to be trends. So, these trends which over  
657 short study periods, without caution, would be imputed easily to climate change may actually only be  
658 sections of slower fluctuation (from internal climate variability) that cannot be evidenced by the length  
659 of the study period. Because large-scale atmospheric and oceanic fluctuations are expressed over a wide  
660 range of timescales, any groundwater trend could be the result of a slower fluctuation (Rossi et al.,  
661 2011). For instance, the Atlantic Multidecadal Oscillation (AMO) oscillates on ~60-yr timescales (Kerr,  
662 2000; Enfield et al., 2001). As mentioned earlier, the age of French piezometric networks does not, in  
663 most cases, allow us to grasp such a low-frequency timescale as a fluctuation in groundwater levels, but  
664 it can be grasped to be trend. To overcome these drawbacks, some studies have used the Ensemble  
665 Empirical Mode Decomposition (EEMD) method to filter out climate variability in precipitation,  
666 streamflow, or meteorological drought signals and detect non-linear trends (Massei and Fournier, 2012;  
667 Sang et al., 2014; Guo et al., 2016; Song et al., 2020). For instance, Massei and Fournier (2012)  
668 concluded that the non-linear trend in the daily Seine River flow could be related to a larger scale NAO  
669 fluctuation, indicating the reversibility of the phenomenon. Therefore, this highlights the complexity to  
670 define whether the trends in hydroclimate variables can be related to climate change or are simply a  
671 portion of some low-frequency fluctuations of large-scale atmospheric or oceanic circulation.

672

673 Without considering the anthropogenic impacts (which data are often poorly referenced), the most  
674 limiting factor for distinguishing a climate change origin of the trend from an internal climate variability  
675 origin (in particular from segments of low-frequency fluctuations that may appear as short-term trends)

676 remains the availability of groundwater level data. Studies on groundwater level reconstruction might  
677 overcome this constraint via, for instance, deep learning approaches or tree-ring-based reconstructions  
678 (Vu et al., 2020; Tegel et al., 2020). However, disentangling climate change and large-scale climate  
679 natural variability would still remain difficult, even with longer time series data, as anthropogenic  
680 forcing may have already impacted climate variability (Dong et al., 2011; Caesar et al., 2018).

681

682 Disentangling the determinism of trends in terms of internal climate variability or climate change lies  
683 behind the scope of the present study. It is rather dedicated to assess how low-frequency variability can  
684 affect trend estimations. Owing to the database used, the trends possibly detected here cannot result  
685 from groundwater abstraction by pumping. However, as this database does not consider changes in land  
686 cover, some trends in groundwater levels could then result from such influence involving recharge  
687 modifications for instance.

688

#### 689 4.2. Catchment and aquifer properties and their impact on variability time scales of 690 groundwater levels

691 The analysis of the spatial distribution of multi-timescale variability revealed the predominance of ~1-  
692 yr, ~7-yr, and ~17-yr variabilities in groundwater levels throughout Metropolitan France. The ~1-yr  
693 variability can be explained by the hydrological cycle (winter recharge and summer recession), while  
694 the ~7-yr and ~17-yr variabilities originate from climatic/oceanic large-scale variability as already  
695 demonstrated by Massei et al. (2010), Massei and Fournier (2012), El Janyani et al. (2012) or more  
696 recently Rust et al. (2019).

697

698 The present study showed that the significance of the low-frequency variability in groundwater levels  
699 is highly variable between French hydrogeological entities. The low-frequency variability can be either  
700 predominant in the total variance of groundwater levels or weakly depicted. These discrepancies are  
701 primarily dependent on intrinsic catchment and aquifer properties such as the permeability and thickness  
702 of the unsaturated zone, the hydrodynamic properties (transmissivity and storage coefficient), the

703 aquifer geometry, the connection with neighbouring aquifers and river system (El Janyani et al., 2012;  
704 Rust et al., 2018).

705

706 Aquifers constituted of rocks with low matrix porosity and highly fractured such as limestones and  
707 bedrock would tend to exhibit groundwater levels dominated by an annual variability and a weak low-  
708 frequency variability due to a high diffusivity. Conversely, aquifers with high storage capacity and  
709 thickness, low transmissivity, and significant thickness of superficial formations such as chalk aquifers  
710 tend to display groundwater levels dominated by multi-annual to decadal variabilities (Slimani et al.,  
711 2009; El Janyani et al., 2012). The exact same behaviour was also recently highlighted by Rust et al.  
712 (2019) in chalk aquifers of Great Britain.

713

714 However, the location in the regional geomorphology (valley, plateau) and hydraulic gradient would  
715 exert a strong control on the significance of multi-annual and decadal variabilities in groundwater levels  
716 (El Janyani et al., 2012), with high-amplitude low-frequency variations for downgradient piezometers.  
717 On the contrary, piezometers with lower amplitudes of low-frequency variations and high amplitudes  
718 of annual variations would be generally found at upgradient locations and then not associated to the  
719 drainage of large areas of subterranean watersheds. Such boreholes would then also be located on  
720 plateau areas, where superficial formations and unsaturated zone are thinner (Slimani et al., 2009). It  
721 then turns out that the geomorphological context and properties such as the presence of superficial  
722 formations, aquifer thickness and transmissivity, but also the location within the hydraulic gradient are  
723 determinant explanatory factors.

724

725 Local conditions would also play a major role in defining the hydrogeological determinism of  
726 groundwater level behaviour. For instance, piezometers located downgradient would correspond to the  
727 drainage of a large volume of aquifer and would then display enhanced low-frequency behaviour, but  
728 in karst areas such boreholes are also very likely associated to highly transmissive karst zones (the so-  
729 called “output karst”) that display strong and fast response to precipitation (i.e., favoring high amplitude  
730 high-frequency variations). The influence of such characteristics on the frequency behaviour of

731 groundwater levels have been successfully put in evidence using a physics-based modeling approach in  
732 the Seine watershed (Schuite et al., 2019).

733

734 On the scale of the whole Metropolitan France area, however, due to the lack of data about physical  
735 properties of aquifers and an insufficient gathering of existing data into a database, it would be hazardous  
736 to get any further into the interpretation of the impact of physical properties on the significance of low-  
737 frequency variabilities in groundwater levels. Hence, the development of such a database gathering the  
738 physical properties of aquifers near boreholes across Metropolitan France would be useful for further  
739 investigations.

740

#### 741 4.3. Influence of multi-annual and decadal variabilities on groundwater trends and 742 comparison with their influence on (effective) precipitation trends

743 Our analyses emphasized the need for long groundwater time series to get better insight into the  
744 existence and meaning of trends regarding the presence of low-frequency variability. Extending the  
745 groundwater time series period by 20 years revealed a decrease in the influence of multi-annual  
746 variability (~7-yr) on trends. Thus, this component only little affected the trend. Obviously, the  
747 significance of this influence also depends on the water table behaviour and thus on the relative  
748 importance of multi-annual or decadal variabilities in the total variance of groundwater levels. The more  
749 the considered variability (multi-annual or decadal) dominates groundwater levels, the more influence  
750 it has on the trend.

751

752 We also noted that some trends carried by either the multi-annual or decadal variability, are caused by  
753 changes in the amplitude of the low-frequency variabilities over time. These regular changes in the  
754 variance of low-frequency variabilities have been highlighted in many precipitation and streamflow  
755 studies (Fritier et al., 2012; Dieppois et al., 2013 and 2016; Massei et al., 2010 and 2017). In the  
756 Normandy chalk, downward trends detected in groundwater levels seem to be partly related to a  
757 weakening of the low-frequency variability over time, the decadal variability appearing to be the main

758 responsible for these downward trends. Its removal largely influenced trends (they became much smaller  
759 in magnitude), whereas that of multi-annual variability did little or not affect trend magnitude. This may  
760 also explain the stable downward trends detected in Normandy chalk and why changing the time series  
761 length has no effect on trend direction.

762

763 In Section 3.3., we demonstrated the significant influence of multi-annual and decadal variabilities on  
764 groundwater level trends. This large influence of such low-frequency variabilities on groundwater trends  
765 raises the following question: is this influence inherent to the aquifer systems, or does it influence trends  
766 of precipitation and effective precipitation in the same way? We thus also analysed these variables to  
767 answer this question.

768

769 In all hydrogeological units of the Paris Basin, the decadal variability drives groundwater levels down  
770 and thus aggravates downward trends over the 1976–2019 period (Fig. 9). Our analyses on precipitation  
771 and effective precipitation showed primarily the same influence of decadal variability on precipitation  
772 and effective precipitation trends as on groundwater levels (Fig. 11). It drives precipitation levels down,  
773 attenuating upward trends and accentuating downward trends. These consistent results indicate that this  
774 influence of decadal variability on groundwater trends is climatologically induced and is not affected  
775 by catchment and aquifer systems.

776

777 **Figure 11.** *Comparison of precipitation trend magnitude between cumulated monthly precipitation,*  
778 *~7-yr filtered cumulated monthly precipitation and ~17-yr filtered cumulated monthly precipitation*  
779 *over 1976–2019;*

780 *a) and b) show precipitation results, c) and d) show effective precipitation results.*

781 *The legend of hydrogeological entities can be found on Figure 8.*

782

783 Our study also revealed a reversal of the effect pattern of multi-annual variability on trends over the  
784 1996–2019 period between aquifers in northern and southern France (Fig. 8). The analysis of  
785 precipitation (P) data showed that over all of France the influence of multi-annual variability on trends

786 is homogeneous: it drives precipitation levels down, attenuating upward trends and accentuating  
787 downward trends (Fig. 12). Thus, the influence of multi-annual variability on trends indicates a reversed  
788 pattern between precipitation and groundwater levels in northern France, particularly in the Paris Basin.  
789 Either potential evapotranspiration (PET) and/or aquifer properties may affect the influence of multi-  
790 annual variability on trends and reverse its effect. However, we observed a similar influence of multi-  
791 annual variability on effective precipitation (EP) trends as on groundwater trends in the Paris Basin,  
792 driving effective precipitation levels up (Fig. 13). Knowing that EP is equivalent to P-PET, this result  
793 suggests that PET would be responsible for this reversal pattern between precipitation and groundwater  
794 levels, rather than catchment and aquifer properties.

795

796 **Figure 12.** *Comparison of precipitation trend magnitude between cumulated monthly precipitation*  
797 *and ~7-yr filtered cumulated monthly precipitation over 1996–2019.*

798

799 **Figure 13.** *Comparison of effective precipitation trend magnitude between cumulated monthly*  
800 *effective precipitation and ~7-yr filtered cumulated monthly effective precipitation over 1996–2019.*

801

802 In southern France, over the 1996–2019 period, the influence of multi-annual variability is the same on  
803 precipitation trends, effective precipitation trends and groundwater trends (Fig. 8, 12 and 13). Only the  
804 Mediterranean region shows atypical results, as the multi-annual variability drives precipitation and  
805 groundwater levels down, while driving effective precipitation levels up. This indicates that, first, PET  
806 would affect the influence of multi-annual variability on trends by reversing the effect between  
807 precipitation and effective precipitation, and second, that catchments and aquifer properties would affect  
808 this influence in turn to reverse it again between effective precipitation and groundwater levels. To better  
809 understand and explain this phenomenon, further investigations will be necessary at a regional scale.

810

811 Over the longer period of 1976–2019, the influence of multi-annual variability on trends of precipitation,  
812 effective precipitation and groundwater levels is heterogeneous in northern France (Fig. 9 and 11). Some  
813 regions (Normandy, Champagne, and Artois-Picardy) show a rather consistent influence of multi-annual

814 variability on trends, regardless of the variable (precipitation, effective precipitation, groundwater  
815 levels). For these regions, the multi-annual variability primarily drives levels up (attenuating downward  
816 trends or accentuating upward trends). In other regions however, such as Bessin, Beauce and Bourgogne,  
817 the available data indicate different influences of multi-annual variability on precipitation, effective  
818 precipitation, and groundwater level trends. We will not extend the discussion to these regions because  
819 the results showed disparities at the local scale.

820

821 Our analysis provides a first insight into the influence of multi-annual and decadal variabilities in  
822 groundwater levels on estimated trends. Generally, the influence of both low-frequency variabilities is  
823 also similar on precipitation and effective precipitation trends. We observe multi-annual and decadal  
824 variabilities that aggravate downward trends or mitigate upward trends either in groundwater,  
825 precipitation and effective precipitation. It is known that low-frequency variability (originating from  
826 internal climate variability) may modulate anthropogenically-driven trends, particularly those induced  
827 by climate change (Kingston et al., 2020). Our result indicates that low-frequency variabilities would be  
828 able to aggravate trends (i.e., amplify downward trends) that might be induced by anthropogenic climate  
829 change. For regions that are already submitted to regular meteorological and hydrological droughts, this  
830 result may be particularly alarming, such as for the Mediterranean region that is defined as an  
831 anthropogenic climate change “hotspot” (Diffenbaugh and Giorgi, 2012; Lionello and Scarascia, 2018;  
832 Drobinski et al., 2020; Trambly et al., 2020). However, even if it is accepted that low-frequency  
833 variability may accentuate, attenuate or inverse the long-term effects of climate change on hydrological  
834 processes (Fatichi et al., 2014; Gu et al., 2019; Massei et al., 2020), our methodology in this article does  
835 not allow us to obtain residual trends that may be only related to climate change. Indeed, we subtracted  
836 individually each low-frequency variability to assess their specific influence on trends and consequently  
837 there is still some low-frequency in residual time series (filtered ones) on which the trend is re-estimated.  
838 Consequently, we do not estimate directly the aggravating or mitigating potential of low-frequency  
839 variability on trends that would be related only to climate change.

840



841 In some areas, however, discrepancies exist between precipitation and effective precipitation, suggesting  
842 the possible influence of PET that inverses the effect of multi-annual variability on trends (over 1996–  
843 2019) in the Paris Basin. Locally, discrepancies can appear between effective precipitation and  
844 groundwater levels, such as in the Beauce area over 1976–2019 due to aquifer properties that  
845 significantly filter the multi-annual variability, which then no longer affects groundwater trends. Further  
846 investigations will be necessary to better understand the processes and physical properties causing the  
847 reversal of the influence of low-frequency variability on trends between precipitation and groundwater  
848 levels.

849

850 The large influence of low-frequency variability on estimated groundwater level trends entails several  
851 implications. First regarding conclusions about traces of climate change in groundwater levels, since  
852 trends may actually correspond to the presence of low-frequency variability, and then be primarily the  
853 result of internal climate variability instead of anthropogenic climate change. Second regarding future  
854 evolutions of groundwater levels, since a potential change in the amplitude of internal climate variability  
855 (that may also be the consequence of anthropogenic climate change) – e.g. increasing or decreasing low-  
856 frequency variability – in the next decades may lead to substantial changes in groundwater level trends.  
857 Consequently, the extrapolation of trends estimated over the historical period seems particularly  
858 hazardous, due to the stochastic and unpredictable behaviour of such low-frequency fluctuations. Third  
859 regarding future projections, because internal climate variability is often improperly reproduced and is  
860 a major source of uncertainties in climate and hydrological projections resulting from GCM outputs  
861 (Terray and Boé, 2013; Qasmi et al., 2017). Consequently, trend estimates resulting from these  
862 hydrological projections (and *in fine* resulting from recharge and groundwater level projections) would  
863 be subject to strong uncertainty.

864

## 865 **5. Conclusion**

866 The analysis of groundwater level trends in France showed that a number of aquifers were susceptible  
867 to trend direction instabilities (i.e., changes in trend direction according to the length of time series),

868 leading to contradictory conclusions about groundwater level evolutions. This led to the question of the  
869 existence, importance and spatial distribution of low-frequency variability in groundwater levels of  
870 French aquifers. Groundwater levels were therefore broken down by MODWT to estimate the  
871 significance of low-frequency variabilities in total groundwater level variability. It turned out that most  
872 of aquifers susceptible to trend direction instabilities exhibit a hydrological variability characterized by  
873 a significant low-frequency variability: they are aquifers with inertial or combined behaviour of water  
874 tables. Given the significant presence of multi-annual and decadal variabilities in groundwater levels,  
875 we aimed to determine if, how and to what extent each of these components could affect trend estimates.  
876 To this end, MODWT filtering was performed to subtract individually the multi-annual or decadal  
877 variability from the entire signal, and then trends were re-estimated on the filtered groundwater level  
878 time series. The results showed that the groundwater level trends were highly sensitive to the presence  
879 of any of these low-frequency components, which may then strongly influence the estimated trends.  
880 Such results indicate that low-frequency variability (originating from internal climate variability) is  
881 capable of attenuating or accentuating groundwater level trends, including those that might be associated  
882 with climate change.

883

884 In general, trend detection is widely used as a tool for assessing changes in groundwater levels.  
885 Nevertheless, our study presents features that show that this tool should be used with caution,  
886 particularly for studying groundwater levels with significant low-frequency variability. We observed  
887 that: (i) trends are highly dependent upon the study period and time series length, and cannot be  
888 extrapolated; (ii) trends are strongly influenced and guided by low-frequency variability, and (iii) trends  
889 are often only segments of larger scale fluctuations resulting from large-scale atmospheric or oceanic  
890 circulation. Consequently, their interpretation and attribution to a physical phenomenon, such as climate  
891 change *vs.* climate variability, remains complex. In addition, since low-frequency variability strongly  
892 guides and influences the estimated groundwater level trends, potential changes in low-frequency  
893 variability – induced by changes in internal climate variability – would necessarily lead to a change in  
894 the estimated trends. In particular, this means that (i) estimation of trends in hydrological projections  
895 resulting from GCM outputs in which low-frequency variability is not well represented would be

896 subject to strong uncertainty, (ii) a potential change in internal climate variability – e.g. increasing or  
897 decreasing low-frequency variability – in the next decades may lead to substantial changes in estimated  
898 groundwater level trends.

899

900 Consequently, future works should focus on assessing the impacts of a potential change in internal  
901 climate variability (i.e., low-frequency variability) on groundwater level trends using different scenarios  
902 of amplitude-modifications of low-frequency variability. In addition, a sensitivity analysis of the results  
903 of this study to decomposition method employed (e.g. wavelets, EEMD) should be conducted.

904

## 905 **Acknowledgments**

906

907 This work was partially supported by the GeoERA project TACTIC, funded by the European Union's  
908 Horizon 2020 research and innovation programme under grant agreement number 731166. We would  
909 also like to thank the AESN and PIREN Seine programs for their support. Finally, we would like to  
910 thank Sandra Lanini for the calculation of effective precipitation; the two anonymous reviewers for their  
911 thoughtful comments that definitely helped improving the paper; Marinus Kluijver for editing the final  
912 English version; Jean-Jacques Seguin, Marc Laurencelle and Laurence Gourcy for the helpful  
913 discussions.

914

## 915 **References**

916 Baulon, L., Allier, D., Massei, N., Bessiere, H., Fournier, M., Bault, V., 2020. Influence de la  
917 variabilité basse-fréquence des niveaux piézométriques sur l'occurrence et l'amplitude des  
918 extrêmes. *Géologues* 207, 53–60.

919 Blöschl, G., Hall, J., Viglione, A., Perdigão, R.A.P., Parajka, J., Merz, B., Lun, D., Arheimer, B.,  
920 Aronica, G.T., Bilibashi, A., Boháč, M., Bonacci, O., Borga, M., Čanjevac, I., Castellarin, A.,  
921 Chirico, G.B., Claps, P., Frolova, N., Ganora, D., Gorbachova, L., Gül, A., Hannaford, J.,

922 Harrigan, S., Kireeva, M., Kiss, A., Kjeldsen, T.R., Kohnová, S., Koskela, J.J., Ledvinka, O.,  
923 Macdonald, N., Mavrova-Guirguinova, M., Mediero, L., Merz, R., Molnar, P., Montanari, A.,  
924 Murphy, C., Osuch, M., Ovcharuk, V., Radevski, I., Salinas, J.L., Sauquet, E., Šraj, M.,  
925 Szolgay, J., Volpi, E., Wilson, D., Zaimi, K., Živković, N., 2019. Changing climate both  
926 increases and decreases European river floods. *Nature* 573, 108–111.  
927 <https://doi.org/10.1038/s41586-019-1495-6>

928 Boé, J., Habets, F., 2014. Multi-decadal river flow variations in France. *Hydrology and Earth System*  
929 *Sciences* 18, 691–708. <https://doi.org/10.5194/hess-18-691-2014>

930 Burn, D.H., Hannaford, J., Hodgkins, G.A., Whitfield, P.H., Thorne, R., Marsh, T., 2012. Reference  
931 hydrologic networks II. Using reference hydrologic networks to assess climate-driven changes  
932 in streamflow. *Hydrological Sciences Journal* 57, 1580–1593.  
933 <https://doi.org/10.1080/02626667.2012.728705>

934 Burn, D.H., Whitfield, P.H., 2018. Changes in flood events inferred from centennial length streamflow  
935 data records. *Advances in Water Resources* 121, 333–349.  
936 <https://doi.org/10.1016/j.advwatres.2018.08.017>

937 Caesar, L., Rahmstorf, S., Robinson, A., Feulner, G., Saba, V., 2018. Observed fingerprint of a  
938 weakening Atlantic Ocean overturning circulation. *Nature* 556, 191–196.  
939 <https://doi.org/10.1038/s41586-018-0006-5>

940 Caporali, E., Lompi, M., Pacetti, T., Chiarello, V., Fatichi, S., 2020. A review of studies on observed  
941 precipitation trends in Italy. *International Journal of Climatology* 41, 1–25.  
942 <https://doi.org/10.1002/joc.6741>

943 Chataigner, J., Michon, J., 2019. Prélèvements quantitatifs sur la ressource en eau (données 2016).  
944 Agence française pour la biodiversité (AFB), 12pp.

945 Constantine, W., Percival, D., 2016. wmtsa: Wavelet Methods for Time Series Analysis. R package  
946 version 2.0-1. <<https://CRAN.R-project.org/package=wmtsa>>.

947 Cornish, C.R., Bretherton, C.S., Percival, D.B., 2006. Maximal Overlap Wavelet Statistical Analysis  
948 With Application to Atmospheric Turbulence. *Boundary-Layer Meteorol* 119, 339–374.  
949 <https://doi.org/10.1007/s10546-005-9011-y>

950 Cornish, C. R., Percival, D. B., Bretherton, C. S., 2003. The WMTSA Wavelet Toolkit for Data  
951 Analysis in the Geosciences. *EOS Trans AGU*. 84(46): Fall Meet. Suppl., Abstract NG11A-  
952 0173

953 Degefu, M.A., Alamirew, T., Zeleke, G., Bewket, W., 2019. Detection of trends in hydrological  
954 extremes for Ethiopian watersheds, 1975–2010. *Reg Environ Change* 19, 1923–1933.  
955 <https://doi.org/10.1007/s10113-019-01510-x>

956 Dieppois, B., Durand, A., Fournier, M., Massei, N., 2013. Links between multidecadal and  
957 interdecadal climatic oscillations in the North Atlantic and regional climate variability of  
958 northern France and England since the 17th century. *Journal of Geophysical Research:*  
959 *Atmospheres* 118, 4359–4372. <https://doi.org/10.1002/jgrd.50392>

960 Dieppois, B., Lawler, D.M., Slonosky, V., Massei, N., Bigot, S., Fournier, M., Durand, A., 2016.  
961 Multidecadal climate variability over northern France during the past 500 years and its  
962 relation to large-scale atmospheric circulation. *International Journal of Climatology* 36, 4679–  
963 4696. <https://doi.org/10.1002/joc.4660>

964 Diffenbaugh, N.S., Giorgi, F., 2012. Climate change hotspots in the CMIP5 global climate model  
965 ensemble. *Climatic Change* 114, 813–822. <https://doi.org/10.1007/s10584-012-0570-x>

966 Dong, B., Sutton, R.T., Woollings, T., 2011. Changes of interannual NAO variability in response to  
967 greenhouse gases forcing. *Clim Dyn* 37, 1621–1641. <https://doi.org/10.1007/s00382-010->  
968 0936-6

969 Drobinski, P., Da Silva, N., Bastin, S., Mailler, S., Muller, C., Ahrens, B., Christensen, O.B., Lionello,  
970 P., 2020. How warmer and drier will the Mediterranean region be at the end of the twenty-first  
971 century? *Reg Environ Change* 20, 78. <https://doi.org/10.1007/s10113-020-01659-w>

972 Dudley, R.W., Hirsch, R.M., Archfield, S.A., Blum, A.G., Renard, B., 2020. Low streamflow trends at  
973 human-impacted and reference basins in the United States. *Journal of Hydrology* 580, 124254.  
974 <https://doi.org/10.1016/j.jhydrol.2019.124254>

975 Edijatno, Michel, C., 1989. Un modèle pluie-débit journalier à trois paramètres. *La Houille Blanche* 2,  
976 113-122. <https://doi.org/10.1051/lhb/1989007>

977 El Janyani, S., Massei, N., Dupont, J.-P., Fournier, M., Dörfliger, N., 2012. Hydrological responses of  
978 the chalk aquifer to the regional climatic signal. *Journal of Hydrology* 464–465, 485–493.  
979 <https://doi.org/10.1016/j.jhydrol.2012.07.040>

980 Enfield, D.B., Mestas-Nuñez, A.M., Trimble, P.J., 2001. The Atlantic Multidecadal Oscillation and its  
981 relation to rainfall and river flows in the continental U.S. *Geophysical Research Letters* 28,  
982 2077–2080. <https://doi.org/10.1029/2000GL012745>

983 Espinosa, L.A., Portela, M.M., 2020. Rainfall Trends over a Small Island Teleconnected to the North  
984 Atlantic Oscillation - the Case of Madeira Island, Portugal. *Water Resour Manage.*  
985 <https://doi.org/10.1007/s11269-020-02668-4>

986 European Commission, 2009. COMMON IMPLEMENTATION STRATEGY FOR THE WATER  
987 FRAMEWORK DIRECTIVE (2000/60/EC) - Guidance Document n°18 - GUIDANCE ON  
988 GROUNDWATER STATUS AND TREND ASSESSMENT – EC 2009, ISBN 978-92-79-  
989 11374-1 - Chap. 5.3.1.

990 Fatichi, S., Rimkus, S., Burlando, P., Bordoy, R., 2014. Does internal climate variability overwhelm  
991 climate change signals in streamflow? The upper Po and Rhone basin case studies. *Science of  
992 The Total Environment* 493, 1171–1182. <https://doi.org/10.1016/j.scitotenv.2013.12.014>

993 Fatichi, S., Molnar, P., Mastrotheodoros, T., Burlando, P., 2015a. Diurnal and seasonal changes in  
994 near-surface humidity in a complex orography. *Journal of Geophysical Research:  
995 Atmospheres* 120, 2358–2374. <https://doi.org/10.1002/2014JD022537>

996 Fossa, M., Dieppois, B., Massei, N., Fournier, M., Laignel, B., Vidal, J.-P., 2021. Spatio-temporal and  
997 cross-scale interactions in hydroclimate variability: a case-study in France. *Hydrology and  
998 Earth System Sciences Discussions* 1–29. <https://doi.org/10.5194/hess-2021-81>

999 Fritier, N., Massei, N., Laignel, B., Durand, A., Dieppois, B., Deloffre, J., 2012. Links between NAO  
1000 fluctuations and inter-annual variability of winter-months precipitation in the Seine River  
1001 watershed (north-western France). *Comptes Rendus Geoscience* 344, 396–405.  
1002 <https://doi.org/10.1016/j.crte.2012.07.004>

1003 Giuntoli, I., Renard, B., Vidal, J.-P., Bard, A., 2013. Low flows in France and their relationship to  
1004 large-scale climate indices. *Journal of Hydrology* 482, 105–118.  
1005 <https://doi.org/10.1016/j.jhydrol.2012.12.038>

1006 Gouhier, T.C., Grinsted, A., 2012. biwavelet: Conduct univariate and bivariate wavelet analyses. R  
1007 package version 0.12. <<http://CRAN.R-project.org/package=biwavelet>>.

1008 Gu, L., Chen, J., Xu, C.-Y., Kim, J.-S., Chen, H., Xia, J., Zhang, L., 2019. The contribution of internal  
1009 climate variability to climate change impacts on droughts. *Science of The Total Environment*  
1010 684, 229–246. <https://doi.org/10.1016/j.scitotenv.2019.05.345>

1011 Gudmundsson, L., Tallaksen, L.M., Stahl, K., Fleig, A.K., 2011. Low-frequency variability of  
1012 European runoff. *Hydrol. Earth Syst. Sci.* 15, 2853–2869. [https://doi.org/10.5194/hess-15-](https://doi.org/10.5194/hess-15-2853-2011)  
1013 [2853-2011](https://doi.org/10.5194/hess-15-2853-2011)

1014 Guo, B., Chen, Z., Guo, J., Liu, F., Chen, C., Liu, K., 2016. Analysis of the Nonlinear Trends and  
1015 Non-Stationary Oscillations of Regional Precipitation in Xinjiang, Northwestern China, Using  
1016 Ensemble Empirical Mode Decomposition. *International Journal of Environmental Research  
1017 and Public Health* 13, 345. <https://doi.org/10.3390/ijerph13030345>

1018 Hamed, K.H., Ramachandra Rao, A., 1998. A modified Mann-Kendall trend test for autocorrelated  
1019 data. *Journal of Hydrology* 204, 182–196. [https://doi.org/10.1016/S0022-1694\(97\)00125-X](https://doi.org/10.1016/S0022-1694(97)00125-X)

1020 Hannaford, J., Buys, G., Stahl, K., Tallaksen, L.M., 2013. The influence of decadal-scale variability  
1021 on trends in long European streamflow records. *Hydrology and Earth System Sciences* 17,  
1022 2717–2733. <https://doi.org/10.5194/hess-17-2717-2013>

1023 Iliopoulou, T., Koutsoyiannis, D., 2020. Projecting the future of rainfall extremes: Better classic than  
1024 trendy. *Journal of Hydrology* 588, 125005. <https://doi.org/10.1016/j.jhydrol.2020.125005>

1025 Kendall, M.G., Stuart, A., Ord, J.K., 1987. Kendall’s advanced theory of statistics. Oxford University  
1026 Press, Inc., USA.

1027 Kerr, R.A., 2000. A North Atlantic Climate Pacemaker for the Centuries. *Science* 288, 1984–1985.  
1028 <https://doi.org/10.1126/science.288.5473.1984>

1029 Kingston, D.G., Massei, N., Dieppois, B., Hannah, D.M., Hartmann, A., Lavers, D.A., Vidal, J.-P.,  
1030 2020. Moving beyond the catchment scale: Value and opportunities in large-scale hydrology

1031 to understand our changing world. *Hydrological Processes* 34, 2292–2298.  
1032 <https://doi.org/10.1002/hyp.13729>

1033 Koutsoyiannis, D., 2006. Nonstationarity versus scaling in hydrology. *Journal of Hydrology* 324, 239–  
1034 254. <https://doi.org/10.1016/j.jhydrol.2005.09.022>

1035 Liesch, T., Wunsch, A., 2019. Aquifer responses to long-term climatic periodicities. *Journal of*  
1036 *Hydrology* 572, 226–242. <https://doi.org/10.1016/j.jhydrol.2019.02.060>

1037 Lionello, P., Scarascia, L., 2018. The relation between climate change in the Mediterranean region and  
1038 global warming. *Reg Environ Change* 18, 1481–1493. [https://doi.org/10.1007/s10113-018-](https://doi.org/10.1007/s10113-018-1290-1)  
1039 1290-1

1040 Lorenzo-Lacruz, J., Vicente-Serrano, S.M., López-Moreno, J.I., Morán-Tejeda, E., Zabalza, J., 2012.  
1041 Recent trends in Iberian streamflows (1945–2005). *Journal of Hydrology* 414–415, 463–475.  
1042 <https://doi.org/10.1016/j.jhydrol.2011.11.023>

1043 McCabe, G.J., Wolock, D.M., 2002. A step increase in streamflow in the conterminous United States.  
1044 *Geophysical Research Letters* 29, 38-1-38-4. <https://doi.org/10.1029/2002GL015999>

1045 Mann, H.B., 1945. Nonparametric Tests Against Trend. *Econometrica* 13, 245–259.  
1046 <https://doi.org/10.2307/1907187>

1047 Massei, N., Dieppois, B., Hannah, D.M., Lavers, D.A., Fossa, M., Laignel, B., Debret, M., 2017.  
1048 Multi-time-scale hydroclimate dynamics of a regional watershed and links to large-scale  
1049 atmospheric circulation: Application to the Seine river catchment, France. *Journal of*  
1050 *Hydrology* 546, 262–275. <https://doi.org/10.1016/j.jhydrol.2017.01.008>

1051 Massei, N., Durand, A., Deloffre, J., Dupont, J.P., Valdes, D., Laignel, B., 2007. Investigating  
1052 possible links between the North Atlantic Oscillation and rainfall variability in northwestern  
1053 France over the past 35 years. *Journal of Geophysical Research: Atmospheres* 112.  
1054 <https://doi.org/10.1029/2005JD007000>

1055 Massei, N., Fournier, M., 2012. Assessing the expression of large-scale climatic fluctuations in the  
1056 hydrological variability of daily Seine river flow (France) between 1950 and 2008 using  
1057 Hilbert–Huang Transform. *Journal of Hydrology* 448–449, 119–128.  
1058 <https://doi.org/10.1016/j.jhydrol.2012.04.052>



1059 Massei, N., Kingston, D.G., Hannah, D.M., Vidal, J.-P., Dieppo, B., Fossa, M., Hartmann, A.,  
1060 Lavers, D.A., Laignel, B., 2020. Understanding and predicting large-scale hydrological  
1061 variability in a changing environment, in: Proceedings of the International Association of  
1062 Hydrological Sciences. Presented at the Hydrological processes and water security in a  
1063 changing world - Hydrological Processes and Water Security in a Changing World, Beijing,  
1064 China, 6–9 November 2018, Copernicus GmbH, pp. 141–149. [https://doi.org/10.5194/piahs-](https://doi.org/10.5194/piahs-383-141-2020)  
1065 [383-141-2020](https://doi.org/10.5194/piahs-383-141-2020)

1066 Massei, N., Laignel, B., Deloffre, J., Mesquita, J., Motelay, A., Lafite, R., Durand, A., 2010. Long-  
1067 term hydrological changes of the Seine River flow (France) and their relation to the North  
1068 Atlantic Oscillation over the period 1950–2008. *International Journal of Climatology* 30,  
1069 2146–2154. <https://doi.org/10.1002/joc.2022>

1070 Mohanavelu, A., Kasiviswanathan, K.S., Mohanasundaram, S., Ilampooranan, I., He, J., Pingale, S.M.,  
1071 Soundharajan, B.-S., Diwan Mohaideen, M.M., 2020. Trends and Non-Stationarity in  
1072 Groundwater Level Changes in Rapidly Developing Indian Cities. *Water* 12, 3209.  
1073 <https://doi.org/10.3390/w12113209>

1074 Morin, E., 2011. To know what we cannot know: Global mapping of minimal detectable absolute  
1075 trends in annual precipitation. *Water Resources Research* 47.  
1076 <https://doi.org/10.1029/2010WR009798>

1077 Neves, M.C., Jerez, S., Trigo, R.M., 2019. The response of piezometric levels in Portugal to NAO,  
1078 EA, and SCAND climate patterns. *Journal of Hydrology* 568, 1105–1117.  
1079 <https://doi.org/10.1016/j.jhydrol.2018.11.054>

1080 Pathak, A.A., Dodamani, B.M., 2019. Trend Analysis of Groundwater Levels and Assessment of  
1081 Regional Groundwater Drought: Ghataprabha River Basin, India. *Nat Resour Res* 28, 631–  
1082 643. <https://doi.org/10.1007/s11053-018-9417-0>

1083 Peña-Angulo, D., Vicente-Serrano, S.M., Domínguez-Castro, F., Murphy, C., Reig, F., Trambly, Y.,  
1084 Trigo, R.M., Luna, M.Y., Turco, M., Noguera, I., Aznárez-Balta, M., García-Herrera, R.,  
1085 Tomas-Burguera, M., Kenawy, A.E., 2020. Long-term precipitation in Southwestern Europe

1086 reveals no clear trend attributable to anthropogenic forcing. *Environ. Res. Lett.* 15, 094070.  
1087 <https://doi.org/10.1088/1748-9326/ab9c4f>

1088 Percival, D.B., Mofjeld, H.O., 1997. Analysis of Subtidal Coastal Sea Level Fluctuations Using  
1089 Wavelets. *Journal of the American Statistical Association* 92, 868–880.  
1090 <https://doi.org/10.1080/01621459.1997.10474042>

1091 Percival, D. B., Walden, A. T., 2000. *Wavelet Methods for Time Series Analysis*. Cambridge  
1092 University Press, Cambridge.

1093 Pérez Ciria, T., Labat, D., Chiogna, G., 2019. Detection and interpretation of recent and historical  
1094 streamflow alterations caused by river damming and hydropower production in the Adige and  
1095 Inn river basins using continuous, discrete and multiresolution wavelet analysis. *Journal of*  
1096 *Hydrology* 578, 124021. <https://doi.org/10.1016/j.jhydrol.2019.124021>

1097 Qasmi, S., Cassou, C., Boé, J., 2017. Teleconnection Between Atlantic Multidecadal Variability and  
1098 European Temperature: Diversity and Evaluation of the Coupled Model Intercomparison  
1099 Project Phase 5 Models. *Geophysical Research Letters* 44, 11,140–11,149.  
1100 <https://doi.org/10.1002/2017GL074886>

1101 Rossi, A., Massei, N., Laignel, B., 2011. A synthesis of the time-scale variability of commonly used  
1102 climate indices using continuous wavelet transform. *Global and Planetary Change* 78, 1–13.  
1103 <https://doi.org/10.1016/j.gloplacha.2011.04.008>

1104 Roux, J.C., 2006. *Aquifères et eaux souterraines en France*. BRGM Editions, 956p.

1105 Rust, W., Holman, I., Bloomfield, J., Cuthbert, M., Corstanje, R., 2019. Understanding the potential of  
1106 climate teleconnections to project future groundwater drought. [https://doi.org/10.5194/hess-](https://doi.org/10.5194/hess-23-3233-2019)  
1107 [23-3233-2019](https://doi.org/10.5194/hess-23-3233-2019)

1108 Rust, W., Holman, I., Corstanje, R., Bloomfield, J., Cuthbert, M., 2018. A conceptual model for  
1109 climatic teleconnection signal control on groundwater variability in Europe. *Earth-Science*  
1110 *Reviews* 177, 164–174. <https://doi.org/10.1016/j.earscirev.2017.09.017>

1111 Sakizadeh, M., Mohamed, M.M.A., Klammler, H., 2019. Trend Analysis and Spatial Prediction of  
1112 Groundwater Levels Using Time Series Forecasting and a Novel Spatio-Temporal Method.  
1113 *Water Resour Manage* 33, 1425–1437. <https://doi.org/10.1007/s11269-019-02208-9>

1114 Sang, Y.-F., Wang, Z., Liu, C., 2014. Comparison of the MK test and EMD method for trend  
1115 identification in hydrological time series. *Journal of Hydrology* 510, 293–298.  
1116 <https://doi.org/10.1016/j.jhydrol.2013.12.039>

1117 Schmockler-Fackel, P., Naef, F., 2010. More frequent flooding? Changes in flood frequency in  
1118 Switzerland since 1850. *Journal of Hydrology* 381, 1–8.  
1119 <https://doi.org/10.1016/j.jhydrol.2009.09.022>

1120 Schuite, J., Flipo, N., Massei, N., Rivière, A., Baratelli, F., 2019. Improving the Spectral Analysis of  
1121 Hydrological Signals to Efficiently Constrain Watershed Properties. *Water Resources*  
1122 *Research* 55, 4043–4065. <https://doi.org/10.1029/2018WR024579>

1123 Sen, P.K., 1968. Estimates of the Regression Coefficient Based on Kendall's Tau. *Biometrika* 63, 1379–1389.  
1124 <https://doi.org/10.1080/01621459.1968.10480934>

1125 Slimani, S., Massei, N., Mesquita, J., Valdés, D., Fournier, M., Laignel, B., Dupont, J.-P., 2009.  
1126 Combined climatic and geological forcings on the spatio-temporal variability of piezometric  
1127 levels in the chalk aquifer of Upper Normandy (France) at pluridecennial scale. *Hydrogeol J*  
1128 17, 1823. <https://doi.org/10.1007/s10040-009-0488-1>

1129 Song, X., Song, Y., Chen, Y., 2020. Secular trend of global drought since 1950. *Environ. Res. Lett.*  
1130 15, 094073. <https://doi.org/10.1088/1748-9326/aba20d>

1131 Stahl, K., Hisdal, H., Hannaford, J., Tallaksen, L., Van Lanen, H., Sauquet, E., Demuth, S.,  
1132 Fendekova, M., Jordar, J., 2010. Streamflow trends in Europe: evidence from a dataset of  
1133 near-natural catchments. *Hydrology and Earth System Sciences* 14, 2367–2382.  
1134 <https://doi.org/10.5194/hess-14-2367-2010>

1135 Stojković, M., Ilić, A., Prohaska, S., Plavšić, J., 2014. Multi-Temporal Analysis of Mean Annual and  
1136 Seasonal Stream Flow Trends, Including Periodicity and Multiple Non-Linear Regression.  
1137 *Water Resour Manage* 28, 4319–4335. <https://doi.org/10.1007/s11269-014-0753-5>

1138 Tegel, W., Seim, A., Skiadaresis, G., Ljungqvist, F.C., Kahle, H.-P., Land, A., Muigg, B., Nicolussi,  
1139 K., Büntgen, U., 2020. Higher groundwater levels in western Europe characterize warm  
1140 periods in the Common Era. *Scientific Reports* 10, 16284. [https://doi.org/10.1038/s41598-](https://doi.org/10.1038/s41598-020-73383-8)  
1141 [020-73383-8](https://doi.org/10.1038/s41598-020-73383-8)

1142 Terray, L., Boé, J., 2013. Quantifying 21st-century France climate change and related uncertainties.  
1143 *Comptes Rendus Geoscience* 345, 136–149. <https://doi.org/10.1016/j.crte.2013.02.003>

1144 Torrence, C., Compo, G.P., 1998. A Practical Guide to Wavelet Analysis. *Bulletin of the American*  
1145 *Meteorological Society* 79, 61–78.  
1146 [https://doi.org/10.1175/1520-0477\(1998\)079<0061:APGTWA>2.0.CO;2](https://doi.org/10.1175/1520-0477(1998)079<0061:APGTWA>2.0.CO;2)

1147 Trambly, Y., Koutroulis, A., Samaniego, L., Vicente-Serrano, S.M., Volaire, F., Boone, A., Le Page,  
1148 M., Llasat, M.C., Albergel, C., Burak, S., Cailleret, M., Kalin, K.C., Davi, H., Dupuy, J.-L.,  
1149 Greve, P., Grillakis, M., Hanich, L., Jarlan, L., Martin-StPaul, N., Martínez-Vilalta, J.,  
1150 Mouillot, F., Pulido-Velazquez, D., Quintana-Seguí, P., Renard, D., Turco, M., Türkeş, M.,  
1151 Trigo, R., Vidal, J.-P., Vilagrosa, A., Zribi, M., Polcher, J., 2020. Challenges for drought  
1152 assessment in the Mediterranean region under future climate scenarios. *Earth-Science*  
1153 *Reviews* 210, 103348. <https://doi.org/10.1016/j.earscirev.2020.103348>

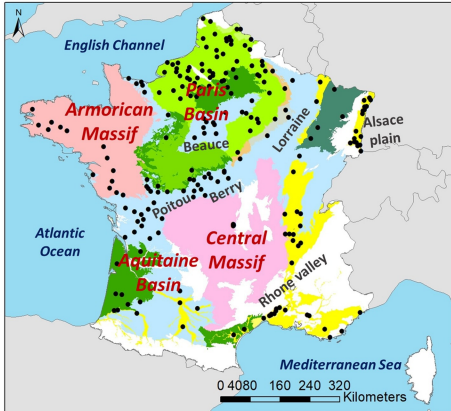
1154 Velasco, E.M., Gurdak, J.J., Dickinson, J.E., Ferré, T.P.A., Corona, C.R., 2017. Interannual to  
1155 multidecadal climate forcings on groundwater resources of the U.S. West Coast. *Journal of*  
1156 *Hydrology: Regional Studies, Water, energy, and food nexus in the Asia-Pacific region* 11,  
1157 250–265. <https://doi.org/10.1016/j.ejrh.2015.11.018>

1158 Vicente-Serrano, S.M., Peña-Gallardo, M., Hannaford, J., Murphy, C., Lorenzo-Lacruz, J.,  
1159 Dominguez-Castro, F., López-Moreno, J.I., Beguería, S., Noguera, I., Harrigan, S., Vidal, J.-  
1160 P., 2019. Climate, Irrigation, and Land Cover Change Explain Streamflow Trends in  
1161 Countries Bordering the Northeast Atlantic. *Geophysical Research Letters* 46, 10821–10833.  
1162 <https://doi.org/10.1029/2019GL084084>

1163 Vidal, J.-P., Martin, E., Franchistéguy, L., Baillon, M., Soubeyroux, J.-M., 2010. A 50-year high-  
1164 resolution atmospheric reanalysis over France with the Safran system. *International Journal of*  
1165 *Climatology* 30, 1627–1644. <https://doi.org/10.1002/joc.2003>

1166 Visser, A., Dubus, I., Broers, H.P., Brouyère, S., Korcz, M., Orban, P., Goderniaux, P., Batlle-Aguilar,  
1167 J., Surdyk, N., Amraoui, N., Job, H., Pinault, J.L., Bierkens, M., 2009. Comparison of

1168 methods for the detection and extrapolation of trends in groundwater quality. *J. Environ.*  
1169 *Monit.* 11, 2030–2043. <https://doi.org/10.1039/B905926A>  
1170 Vu, M.T., Jardani, A., Massei, N., Fournier, M., 2020. Reconstruction of missing groundwater level  
1171 data by using Long Short-Term Memory (LSTM) deep neural network. *Journal of Hydrology*  
1172 125776. <https://doi.org/10.1016/j.jhydrol.2020.125776>



### Legend

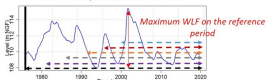
- Groundwater level observation wells

#### Aquifer group

- Bedrock
- Chalk
- Greensands
- Limestones
- Not studied formations
- Sand
- Sandstones
- Volcanic formations
- Alluvial formations

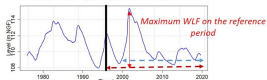
**(a)****Step 1 : a. Assessment of Sen's slope; b. Normalisation by maximum WLF; c. Assignment to a magnitude class**

Reference period : 1976-2019



Well		1976-2019	1981-2019	1986-2019	1991-2019	1996-2019	2000-2019
Xn	Sen's slope						
	Sen/WLF						
	Class						

Reference period : 1996-2019



Well		1996-2019	2000-2019
Xn	Sen's slope		
	Sen/WLF		
	Class		

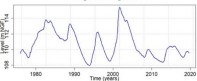
**Step 2 : Class comparison**

Well		1976-2019	1981-2019	1986-2019	1991-2019	1996-2019	2000-2019	Sign stability	Class stability
Xn	Class	Strong ↘	Strong ↘	Strong ↘	Moderate ↘	Strong ↘	Strong ↘	Still ↘	Unstable

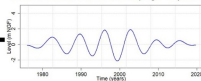
Well		1996-2019	2000-2019	Sign stability	Class stability
Xn	Class	Strong ↘	Strong ↘	Still ↘	Stable

**(b)****Step 1 : Subtraction of the time scale of interest**

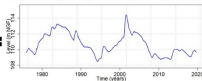
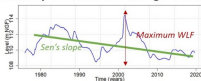
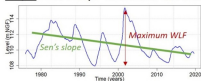
Original signal

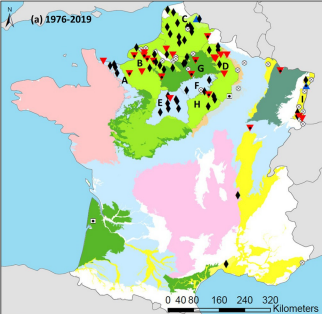


Wavelet detail subtracted (e.g. ~7 years)



Filtered signal of the ~7 years time scale

**Step 2 : Sen's slope calculation and normalisation by maximum WLF of original data**

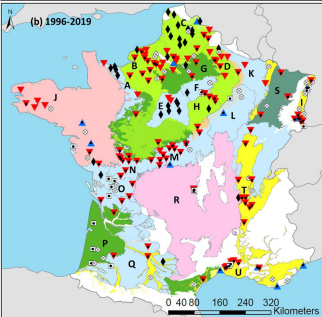


## Legend

- Trend magnitude stability** Aquifer group
- Stable trend class
- Trend direction stability**
- ▲ Still upward trend
  - Still insignificant trend
  - ▼ Still downward trend
  - ◆ Change of sign
  - Emerging trend
- Aquifer group**
- Alluvial formations
  - Bedrock
  - Chalk
  - Greensands
  - Limestones
  - Sand
  - Sandstones
  - Volcanic formations
  - Not studied formations

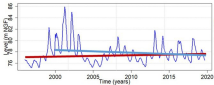
## Hydrogeological entities

- A Jurassic limestones from Sarthe to Bessin
- B Seno-Turonian chalk of Normandy/Picardy
- C Seno-Turonian chalk of Artois-Picardy
- D Seno-Turonian chalk of Champagne
- E Limestones of Beauce
- F Upper Eocene limestone of Paris Basin
- G Lutetian and Ypresian sands of Paris Basin
- H Upper Cretaceous chalk of Bourgogne
- I Alluvial formations of Alsace
- J Bedrock of Brittany
- K Jurassic limestones of Lorraine
- L Jurassic limestones of Côte-des-Bars
- M Jurassic limestones of Berry
- N Jurassic limestones of Poitou
- O Fractured Jurassic limestones of northern Aquitaine Basin
- P Plio-Quaternary sands of Aquitaine Basin
- Q Various calcareous formations of Aquitaine Basin
- R Volcanic formations of Central Massif
- S Triassic sandstones and limestones of Lorraine
- T Fluvio-glacial formations of Rhone valley
- U Alluvial formations of Mediterranean region





## Beauval



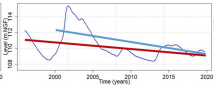
### 1996-2019 :

- Sen's slope = 0.2 cm/month
- Slope/WLF = 10% of WLF

### 2000-2019 :

- Sen's slope = -0.3 cm/month
- Slope/WLF = -13% of WLF

## Goupillieres



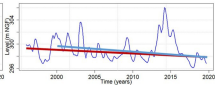
### 1996-2019 :

- Sen's slope = -0.7 cm/month
- Slope/WLF = -43% of WLF

### 2000-2019 :

- Sen's slope = -1.5 cm/month
- Slope/WLF = -76% of WLF

## Penol

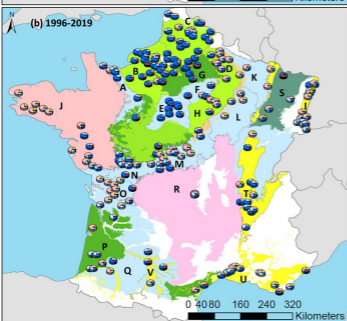
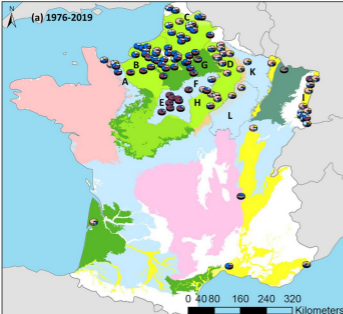


### 1996-2019 :

- Sen's slope = -0.4 cm/month
- Slope/WLF = -15% of WLF

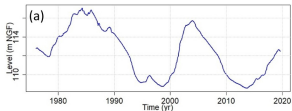
### 2000-2019 :

- Sen's slope = -0.6 cm/month
- Slope/WLF = -19% of WLF

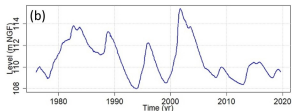


### *Limestones of Beauce*

**Inertial**

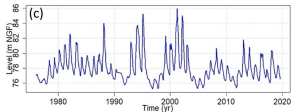


### *Seno-Turonian chalk of Normandy*

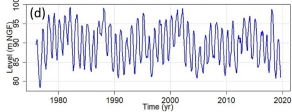


### *Seno-Turonian chalk of Artois-Picardy*

**Combined**

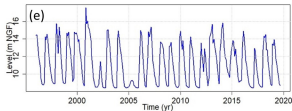


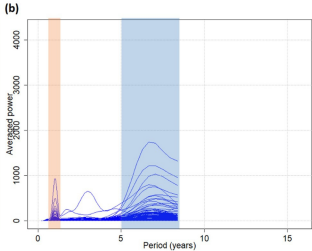
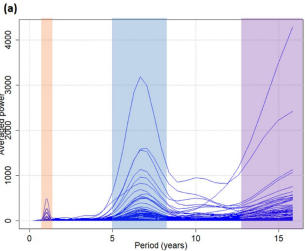
### *Seno-Turonian chalk of Champagne*



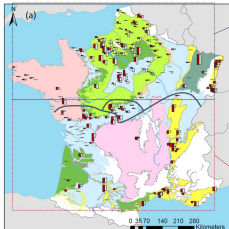
### *Jurassic limestones of northern Aquitaine Basin*

**Annual**

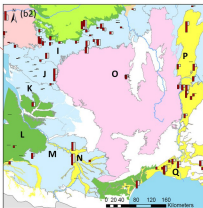
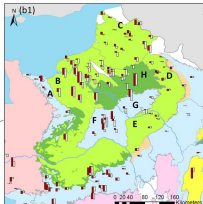




↗ ~7 years timescale drives upward groundwater levels



↘ ~7 years timescale drives downward groundwater levels



Ratio Sen's slope/maximum WLF



■ Raw groundwater levels (monthly averages)

□ 7yrs filtered groundwater levels

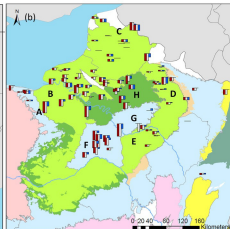
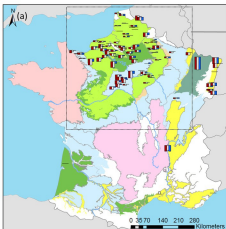
~ Pattern reversal boundary

### Aquifer group

- Bedrock
- Chalk
- Greensands
- Limestones
- Not studied formations
- Sand
- Sandstones
- Volcanic formations
- Alluvial formations

### Hydrogeological entities

- A Jurassic limestones from Sarthe to Bessin
- B Seno-Turonian chalk of Normandy/Picardy
- C Seno-Turonian chalk of Artois-Picardy Basin
- D Chalk of Champagne
- E Upper Cretaceous chalk of Bourgogne
- F Limestones of Beauce
- G Eocene limestones of Paris Basin
- H Lutetian and Ypresian sands of Paris Basin
- I Jurassic limestones of Poitou
- J Fractured Jurassic limestones of northern Aquitaine Basin
- K Upper Cretaceous limestones of Angoumois
- L Plio-Quaternary sands of Aquitaine Basin
- M Calcareous formations of Aquitaine Basin
- N Alluvial formations of Garonne
- O Volcanic formations of Central Massif
- P Fluvio-glacial formations of Rhone valley
- Q Alluvial formations of Mediterranean region



### Ratio Sen's slope/maximum WLF

(a)



(b)



■ Raw groundwater levels (monthly averages)

■ 7yrs filtered groundwater levels

■ 17yrs filtered groundwater levels

### Aquifer group

■ Bedrock

■ Chalk

■ Greensands

■ Limestones

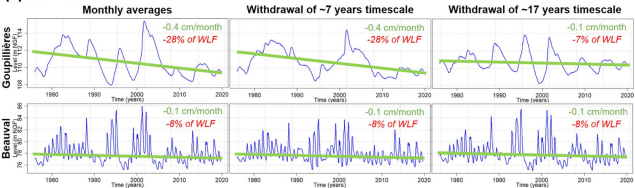
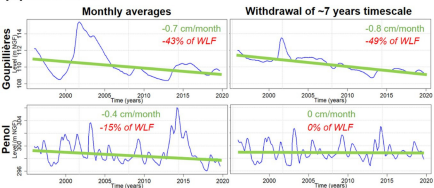
■ Not studied formations

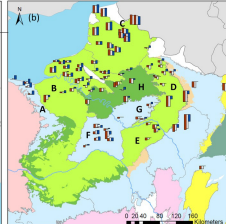
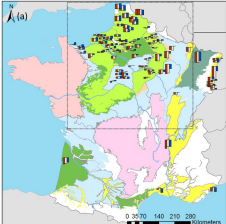
■ Sand

■ Sandstones

■ Volcanic formations

■ Alluvial formations

**(a) 1976-2019****(b) 1996-2019**



Sen's slope (mm/months)

Precipitation



Raw precipitation

7-yr filtered precipitation

17-yr filtered precipitation

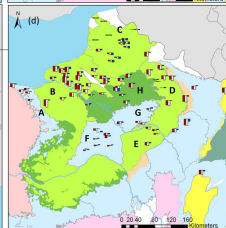
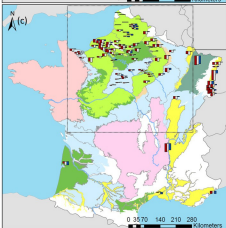
Effective precipitation



Raw effective precipitation

7-yr filtered effective precipitation

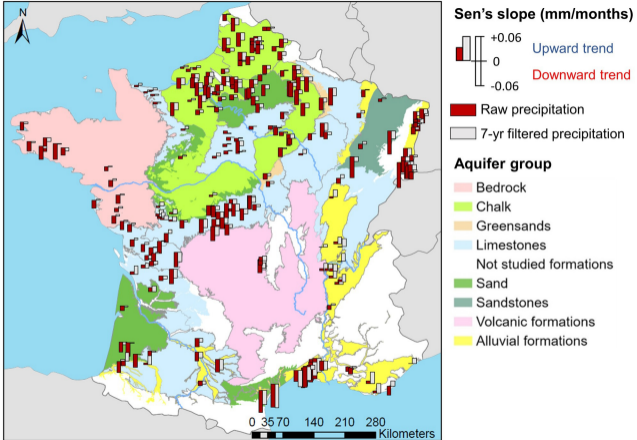
17-yr filtered effective precipitation

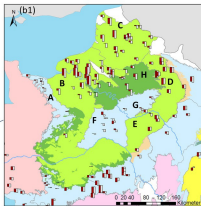
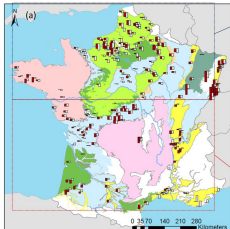


**Aquifer group**

- Bedrock
- Chalk
- Greensands
- Limestones
- Not studied formations
- Sand
- Sandstones
- Volcanic formations
- Alluvial formations







### Aquifer group

- Bedrock
- Chalk
- Greensands
- Limestones
- Not studied formations
- Sand
- Sandstones
- Volcanic formations
- Alluvial formations

### Hydrogeological entities

- A Jurassic limestones from Sarthe to Bessin
- B Seno-Turonian chalk of Normandy/Picardy
- C Seno-Turonian chalk of Artois-Picardy Basin
- D Chalk of Champagne
- E Upper Cretaceous chalk of Bourgogne
- F Limestones of Beauce
- G Eocene limestones of Paris Basin
- H Lutetian and Ypresian sands of Paris Basin
- I Jurassic limestones of Poitou
- J Fractured Jurassic limestones of northern Aquitaine Basin
- K Upper Cretaceous limestones of Angoumois
- L Plio-Quaternary sands of Aquitaine Basin
- M Calcareous formations of Aquitaine Basin
- N Alluvial formations of Garonne
- O Volcanic formations of Central Massif
- P Fluvio-glacial formations of Rhone valley
- Q Alluvial formations of Mediterranean region